2021

Enhancement and Evaluation of Proton Pencil Beam Spot Placement Algorithms

Mahboob Ur Rehman
University of Central Florida

ENHANCEMENT AND EVALUATION OF PROTON PENCIL BEAM SPOT PLACEMENT ALGORITHMS

by

MAHBOOB UR REHMAN
M.S. University at Albany SUNY, Albany, New York, 2015
M.S. Pakistan Institute of Eng. & Appl. Science, Islamabad, Pakistan, 2004

A dissertation submitted in partial fulfillment of the requirements
of the degree of Doctor of Philosophy
in the Department of Physics
in the College of Sciences
at the University of Central Florida
Orlando, Florida

Spring Term
2021

Major Professors: Talat Shahnaz Rahman, Omar Zeidan

ABSTRACT

Intensity modulated proton therapy (IMPT) in the form of pencil beam scanning (PBS) has shown improvement in treatment plan quality as compared to conventional proton and photon-based radiotherapy techniques. However, in IMPT maintaining a sharp lateral dose falloff is crucial for sparing organs at risk (OARs), especially when they are in close proximity to the target volume. The most common approach to improve lateral dose falloff is through the use of physical beam shaping devices, such as brass apertures or collimator-based systems. This work has shown that IMPT can be further improved by implementation of advanced spot placement techniques by moving away from traditional grid-based placements to boundary contoured techniques.

We have developed a new optimized spot placement algorithm that provides robust spot distributions inside the target volume by making use of various geometric construction techniques in other fields and developed a unique spot placement technique that provides both high conformality and uniformity in a robust manner for arbitrarily complex target geometries. This approach achieves the boundary conformity of a recently proposed concentric-contours based approach and uses a fast-iterative method to distribute the interior spots in a highly uniform fashion in an attempt to improve both the lateral dose falloff and uniformity.

We performed the treatment plan quality comparison for five spot placement techniques using customized homogeneous phantoms. These include two grid-based (rectilinear/hexagonal) and three boundary-contoured (concentric-contours, hybrid and optimized) techniques. Treatment plans were created for two different target volumes, (conical and spherical). An optimal set of planning parameters was defined for all treatment plans and the impact of spot placement

techniques on the plan quality was studied in terms of lateral & distal dose falloff, normal tissue sparing, conformity & homogeneity of dose distributions, and total number of spots.

For grid-based spot placement techniques, dose conformity is dependent on the target cross sectional shape, which changes for each proton energy. This variable conformity problem is shown to be mitigated by using boundary contoured techniques. However, in the case of concentric contours, the conformity is improved but at the cost of decreased homogeneity. Hybrid and optimized spot placement techniques show more uniform dose distributions while maintaining the improved dose conformity. The optimized spot placement technique is shown to provide robust treatment plans with improved target coverage, homogeneity of dose, and minimal spots count. These results highlight that plan quality in PBS proton therapy may be improved for many patients, without the need for expensive delivery equipment updates, simply by providing additional spot placement techniques in commercial treatment planning software (TPS).

To my father, Mirza Muhammad Rashid (1945-2013)

Through your love and support you imparted courage to achieve goals in my life.

To my mother, Kaneez Fatima

Your prayers keep me moving in life.

ACKNOWLEDGEMENTS

All praises are due to Allah (SWT), for uncountable blessings, who is the most gracious and the most merciful. I would like to take this opportunity to express my sincere gratitude to my advisor Professor Talat S. Rahman for her patience, motivation, and guidance. I have been fortunate enough to learn not only about research but also about the importance of commitment, discipline, and hard work in life.

I am grateful to Dr. Sanford Meeks and Dr. Patrick Kelly from Orlando Health Cancer Institute for giving me the opportunity to do the doctoral research in their research team. I was lucky to have Dr. Omar Zeidan (Orlando Health Cancer Institute) and Dr. Kevin Erhart (.decimal LLC, Sanford, Florida) as my mentors. They provided me with opportunity to be exposed with the full range of skills related to the proton therapy. They have been very nice and helpful to me throughout my PhD. I am especially grateful to Dr. Kevin Erhart for being there through thick and thin and for providing much appreciated guidelines for my research. He kept me motivated during difficult phases of this journey. It was because of this platform that I was able to complete my CAMPEP accredited certificate from Florida Atlantic University. I would like to acknowledge the financial support for this work from .decimal LLC, Sanford Florida and Florida High Tech. Corridor.

I would also like to extend my heartful thanks to the chair of the Physics Department, Dr. Eduardo Mucciolo, for his continuous efforts in making this project complete. I would like to express my thanks to my committee members Dr. Bhattacharya, Dr. Bo Chen, Dr. Flitsiyan for helping me to achieve my PhD goals. I am also thankful to Ms. Esperanza Soto and Ms. Nikitta Campbell for providing me their help at every step to deal with all different types of administrative barriers.

I wish to thank my wife Madiha Ashfaq, who has stood by me through all my travails, my absences, my fits of pique and impatience. She gave me support and help, discussed ideas and prevented several wrong turns. She also supported the family during my graduate studies. My kids Abdul Rehman, Abdul Moiz, Jawahir Fatima always motivated me through their innocent words and at the same time I welcome our family's new member Rayah Fatima.

The saying "it takes a village to raise a child" is true for a Ph.D. as well. I would like to thank all my teachers and great scientists Dr. M. Sajjad Alam and Dr. Khalid Jamil that kindled the love of knowledge in me. I am grateful to all my past and present colleagues for their well wishes and motivation. I would like to thank Dr. Leventouri, Dr. Wazir Muhammad, Dr. Charles Shang (South Florida Proton Therapy Institute), Dr. Jahangir Satti (Albany Medical Center), Dr. Abbas and Dr. Abrar Hussain for their guidance and motivation.

I would like to acknowledge the support of all my friends, including Naseem ud Din, Asim Ghalib, Junaid Khan, Syed Jaffer, Muhammad Tayyab, Sajid, Saad, Rehan and Sarfaraz Hussain for their companionship during these years. I would also like to thank my friends Nadeem Siddiqui and Nadeem Qureshi for their care and motivation during my difficult times. My friend Asim Janjua has always been with me during this journey and he never let me feel alone. I appreciate my friends Atdhe, Shreen and Maryam from Florida Atlantic University for sharing with wonderful time during the certificate program.

Last but most important, I would like to acknowledge the unconditional love and efforts of my family. My mother and my sisters always encouraged me to work harder. My father passed away after I came for the PhD but today, I acknowledge this degree to him. My younger brothers Habib

ur Rehman and Aziz ur Rehman, my nephew Atiq ur Rehman and my friends Zeshan, Ijaz and Lala have always been a source of motivation to me and I am thankful to them for taking care of my mother after the death of my father. My brother-in-law, Ehsanullah, has always been affectionate to me and helped me whenever I was in difficult situation. I am also thankful to brothers Siddique and Zubair, my nephews and nieces and my in-laws for their moral support during this journey.

TABLE OF CONTENTS

LIST OF FIGURES

LIST OF TABLES

CHAPTER 1: INTRODUCTION

1.1 An Overview and Historical Perspective of Proton Therapy

According to the World Health Organization, cancer has been a leading cause of death all over the world leading to 10 million deaths in 2020 [1]. The primary goal towards treatment of cancer is to cure the disease or to prolong the life span. In both cases, radiation therapy may be used as the sole treatment or in combination with other modalities like surgery and chemotherapy. The history of radiation therapy can be tracked to soon after the discovery of x-rays in 1895. It was observed that radiation can cause cutaneous burns and doctors started using radiation to treat different abnormal growths and lesions. Radiation therapy is generally performed in one of the two ways. Brachytherapy, in which a radiation source is placed precisely at the site of the tumor, or external beam radiotherapy, which involves use of high energy photons/charged particles to deliver radiation dose to the tumor site.

The goal of radiotherapy has always been to deliver maximum radiation dose to the target tumor while sparing the normal tissues. There are continuous efforts in the field of radiotherapy to improve the quality of treatment of cancer patients. Many advanced and sophisticated radiotherapy technologies have been established so far. These new technologies are required to be compared and tested against the existing best available technologies so that merits and demerits can be highlighted before adopting them. Charged Particle Radiation Therapy is one of these technologies which has not been adopted by most part of the world so far. One hundred and ten (110) fully operational particle therapy centers exist in all over the world while thirty-seven (37) are under construction by the end of 2020. The number of particle therapy centers under planning stages is

twenty-eight (28). Most of these centers have proton therapy facility and few with heavy ion therapy like Carbon ions [2]. Charged particle radiation therapy is a special type of radiation therapy in which charged particles (electrons, protons, or heavier ions) are used for treatment of cancer. Electrons are used for the tumors at shallower depths, however for deep seated tumors, protons and other heavy charged particles are used. The most commonly used heavy charged particle for the radiotherapy purposes is the Proton.

Proton is a positively charged sub-atomic particle and its discovery is credited to Ernest Rutherford in 1929 when he concluded that the positively charge in his experiment was the nucleus of a hydrogen atom. The idea for the radiological use of proton was first presented by Robert Wilson that an accelerated proton beam can treat a deep-seated tumor inside the human body. He not only proposed the biophysical basis of the proton beam but also explained the techniques for the beam delivery [3, 4]. The first human treatment was performed using a high energy proton beam at Lawrence Berkeley Laboratory (LBL) in 1954 [5]. Till now, several institutes have been contributing towards the use of charged particles for radiotherapy. The main institutes are: Lawrence Berkeley Laboratory, Harvard Cyclotron Laboratory, Massachusetts General Hospital, Paul Sherrer Institute (PSI), Switzerland. Additionally, physicists in several institutes in other parts of the world have contributed to the development of other key technologies including accelerator technology, magnetically scanned beams and high quality treatment planning systems (TPS), computed tomography imaging systems and magnetic resonance imaging systems. Collectively, these technologies have revolutionized the treatment of cancer with the use of particle therapy. According to ICRU 78, by the end of 2007, there were only 35 functional particle therapy centers

in the world and by the end 2020, according to PTCOG this number has increased to one hundred and ten (110) fully functional particle therapy centers in the world [4-6].

1.2 Rationale of Proton Therapy

The rationale of using proton beams in radiation therapy is based on their physical characteristics when they penetrate matter. These physical characteristics are: i) finite depth of penetration in the material, ii) relatively low ionization density (energy loss per unit length) at the surface but highest ionization density in the small region at the end of the range and iii) the rapid dose fall off at the end of the range[6].

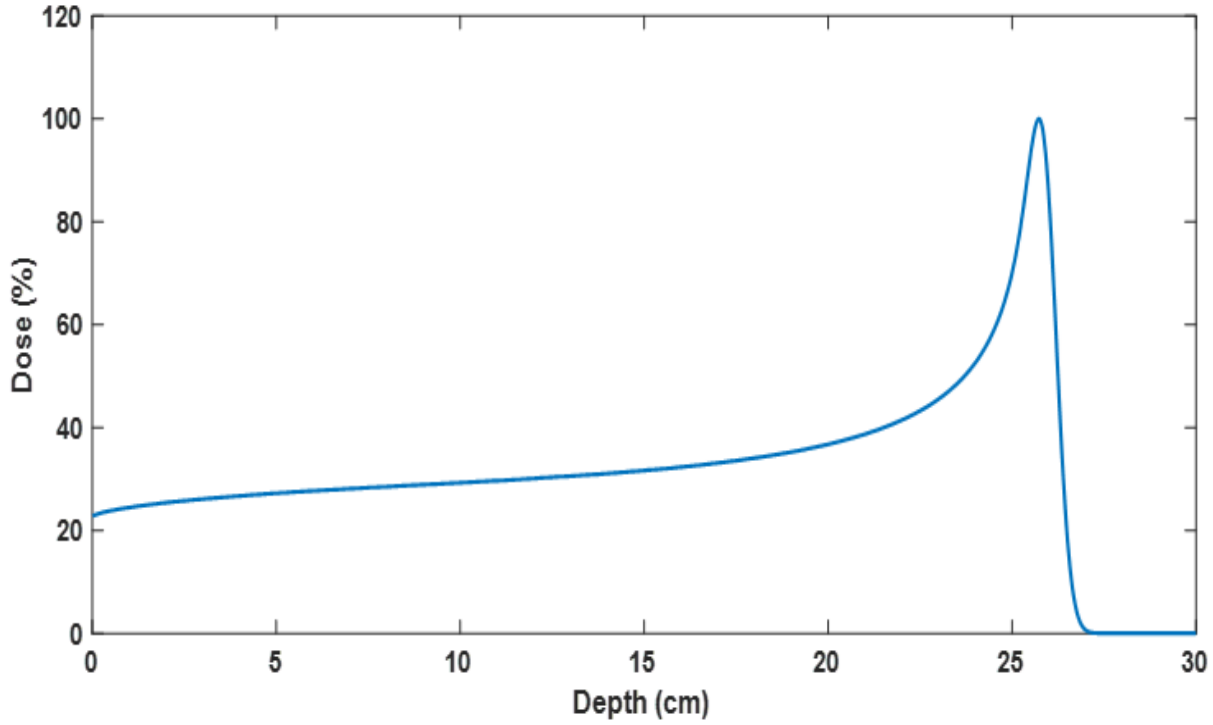

Figure 1.1: Shape of a pristine Bragg Peak created in MATLAB for 200 MeV in water

The depth dose curve of the proton beam is called the “Bragg Curve” after an Australian physicist, William Bragg, worked on the range of proton beam and found the large increase in energy deposition at the end of the beam’s range [7]. The peak in the Bragg curve is called as Bragg Peak (Figure 1.1). The finite range of protons in medium is one of the most important characteristics of the proton beam that can be used in radiation therapy to deliver maximum dose to the target tumor and minimum dose to the surrounding tissues including OARs (Figure (1.2)).

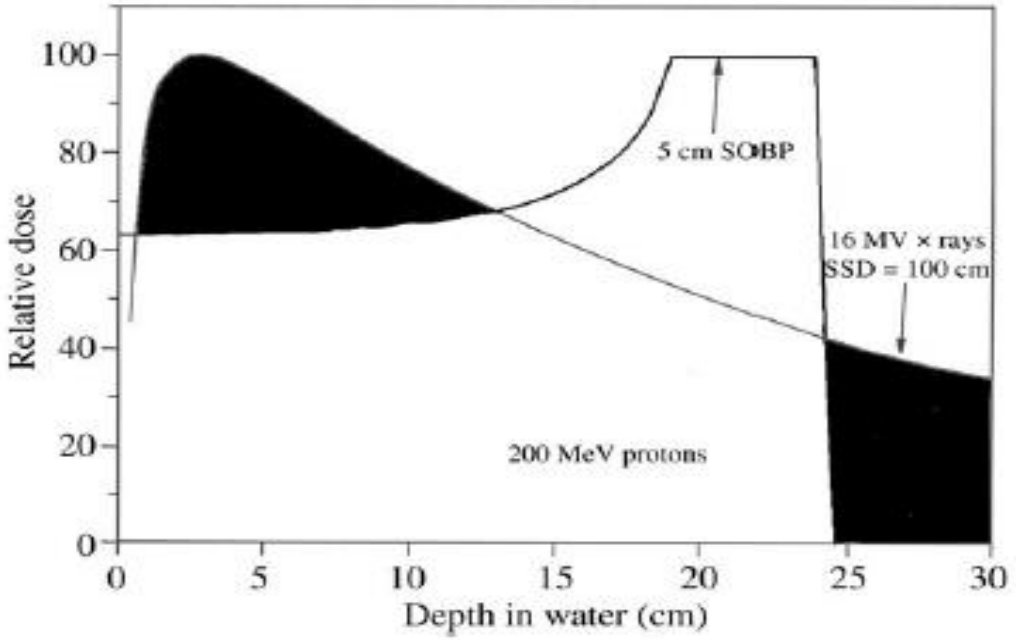

Figure 1.2: Comparison of proton therapy and conventional photon therapy [8]

At the same time, the Bragg Curve of a proton beam can be exploited to enhance the treatment quality by providing less entrance dose and no exit dose as compared to conventional radiotherapy using photon beams, as shown in Figure 1.2 [6, 9]. In the case of proton therapy, dose sparing can be achieved both proximally and distally as compared to conventional radiotherapy using photons

on their depth dose characteristics as shown in Figure 1.2. Literature also shows that there is a reasonable decrease in the probability of the development of secondary malignancies when using the proton beam than the photon beams [6, 10].

1.3 Interaction of Protons with matter

Classically, the interaction of protons with matter is characterized by two basic parameters: 1) the impact parameter ‘b’ and 2) the atomic radius ‘a' and these two parameters define the following three types of interactions [4, 11]:

- Soft Collisions (in-elastic Coulomb Interactions) when b >> a
- Hard Collisions (Coulomb Elastic Scattering) when b ≈ a
- Nuclear Interaction (Non-elastic Nuclear Interaction) when b << a

Through soft collisions with the surrounding electrons of the absorber, protons continuously lose their kinetic energy and slow down. Such approximation is referred as Continuous Slowing Down Approximation (CSDA) and is described by Bethe-Bloch theory that is used to define the range of the proton beam in the medium [4, 11]. In case of elastic Coulomb Scattering (b ≈ a), the interaction target is the nucleus and it causes changes in the trajectory of the proton. Such interactions define the lateral penumbral sharpness in the proton therapy. In case of the non-elastic nuclear interactions, secondary protons, heavier ions, neutrons, and gamma rays are created. The dosimetric manifestation of these interactions is that they define primary fluence of the protons and also causes the generation of stray neutrons and the generation of prompt gammas for in vivo study. However, the deflection of the incident protons from the nucleus field causes a negligible dosimetric effect in terms of energy loss and change in the incident proton trajectory [4, 7, 11].

Protons lose part of their energy primarily through the Coulombic interactions with the atomic electrons of the medium. The rate of loss of energy of all charged particles is defined in terms of the ratio between dE and dx, where dE is the mean energy loss of the proton and dx is the depth traversed in the medium and the ratio was given a name of "Linear Stopping Power" and is attributed to Bohr [7, 12, 13]. The more convenient way to express the linear stopping power is in terms of the quantity S/p called "Mass Stopping Power" with the units of (MeV-cm^2/g) and is given by the equation:

$$\frac{S}{\rho} = -\frac{1}{\rho}\left(\frac{dE}{dx}\right)$$

There are three main contributors to the Mass Stopping Power and therefore, the mass stopping power for protons is written as the sum of those three contributors.

$$\frac{S}{\rho} = -\frac{1}{\rho}\left[\left(\frac{dE}{dx}\right)_{el} + \left(\frac{dE}{dx}\right)_{nuc} + \left(\frac{dE}{dx}\right)_{rad}\right]$$

The first term represents the electronic contribution of the target medium in the mass stopping power. The second term represents the nuclear contribution, and the third term represents the energy loss due to radiations emitted (i.e. radiative contribution) in the Mass stopping power. More accurate formula describing the electronic stopping power and accounting for quantum mechanical effects is attributed to Bethe and Bloch [7, 14, 15].

$$\left(-\frac{dE}{dx}\right)_{el} = 2\pi r_e^2 m_e c^2 N_A \rho \frac{Z}{A}\frac{z^2}{\beta^2}\left[ln\left(\frac{2m_e\gamma^2\vartheta^2 W_{max}}{I}\right) - 2\beta^2 - 2\frac{C}{Z} - \delta\right]$$

Where

N_A	Avogadro's number
r_e	Classical electron radius
m_e	Mass of an electron
z	Charge of the projectile
Z	Atomic number of the absorbing material
A	Atomic weight of the absorbing material and
I	Mean excitation potential of the absorbing material.

Above equation shows the importance of using mass stopping power because of the strong dependence on density. In case of proton therapy, water is considered an equivalent material to the human tissue in terms of the energy loss, multiple coulomb scattering, and the nuclear interactions. Therefore, water is recommended for the phantom material for dose and range measurements and as a reference material to report the other radiotherapy quantities [4, 7, 13].

The range energy relationship of the protons (Figure 1.3) shows that the range of a proton beam increases with the increase in energy. So, different energy proton beams can be used to treat cancer at different depths of the body. Depth and position of the Bragg peak is a function of the beam energy and the material (tissue) in the beam path. Therefore, to be able to irradiate all possible target volumes in an adult patient, proton ranges of 26-38 cm in tissue are required that correspond to proton energies of 200 MeV to 250 MeV [8].

The range of the proton particles increases with the increase in energy [8]. The range-energy relationship of a typical proton beam is shown in Figure 1.3 taken from the International Commission of Radiological Units report number 49 (ICRU 49). So, different energy proton beams can be used to treat cancer at different depths of the body. Depth and position of the Bragg peak

is a function of the beam energy and the material (tissue) heterogeneity in the beam path and to be able to irradiate all possible target volumes in an adult patient, proton ranges of 26-38 cm in tissue are required that correspond to proton energies of 200 MeV to 250 MeV.

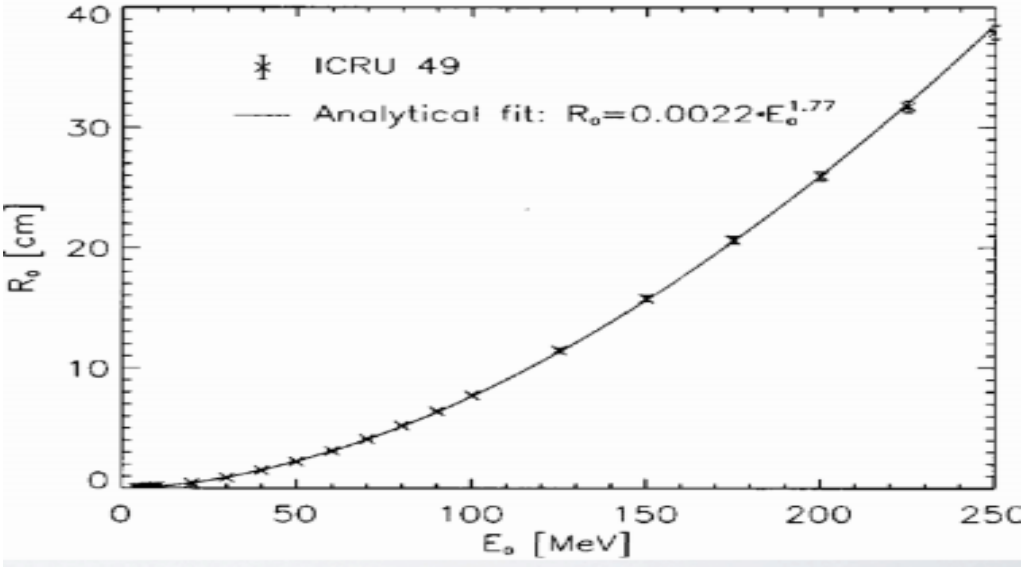

Figure 1.3: Change of range of the proton pencil beam with increase in energy [8]

Figure 1.4 explains different characteristics of a typical proton Bragg curve. This Bragg curve was produced using a MATLAB code for an energy of 200 MeV in-air. One of the most important characteristics of the proton beam is its range. Sometimes it is also called the mean range. It is defined as the range of a proton beam (R_{80}) that corresponds to 80% dose level in the distal fall-off of a depth-dose profile. Similarly, clinical range R_{90} corresponds to the 90% dose level in the distal dose fall-off of the depth dose profile shown in Figure 1.4 [4, 16]. Similarly, practical range is defined as the 10% dose level in the distal dose fall-off direction which can be used to define the residual range as follows:

$$R_{res} = R_p - z$$

Where, R_{res} is the residual range and z is the measurement depth. Bragg peak width is another important parameter shown in Figure 1.4 and it is defined as the width of the 80% dose level.

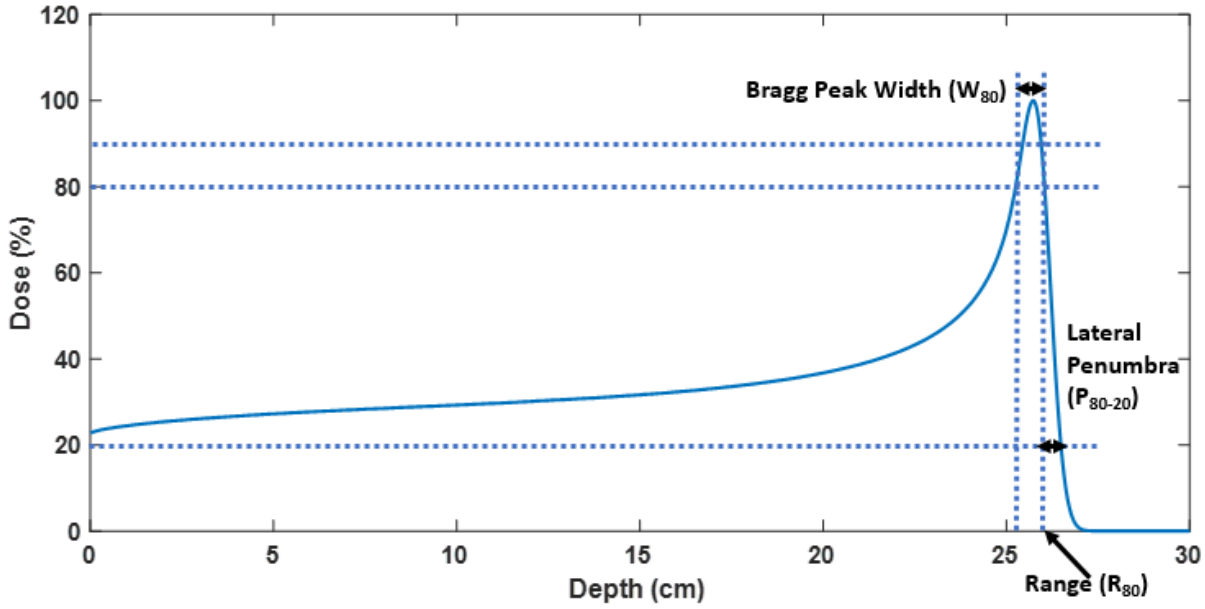

Figure 1.4: Bragg curve created in MATLAB for 200 MeV in air showing important parameters of a Bragg curve used in treatment planning

1.4 Proton Beam Delivery Techniques

Typical proton beams have a lateral spread of only few millimeters when they come out of the accelerator head and therefore the dose distribution of such beam is not clinically useful. Clinical use of the proton beam requires a beam spread in both lateral and transverse directions of the beam. So, to paint the whole tumor volume with the radiation dose, the proton beam needs to be broadened along and perpendicular to the direction of the beam. The modification in the proton beam characteristics can be performed either by 1) Passive Scattering or by 2) Pencil Beam scanning.

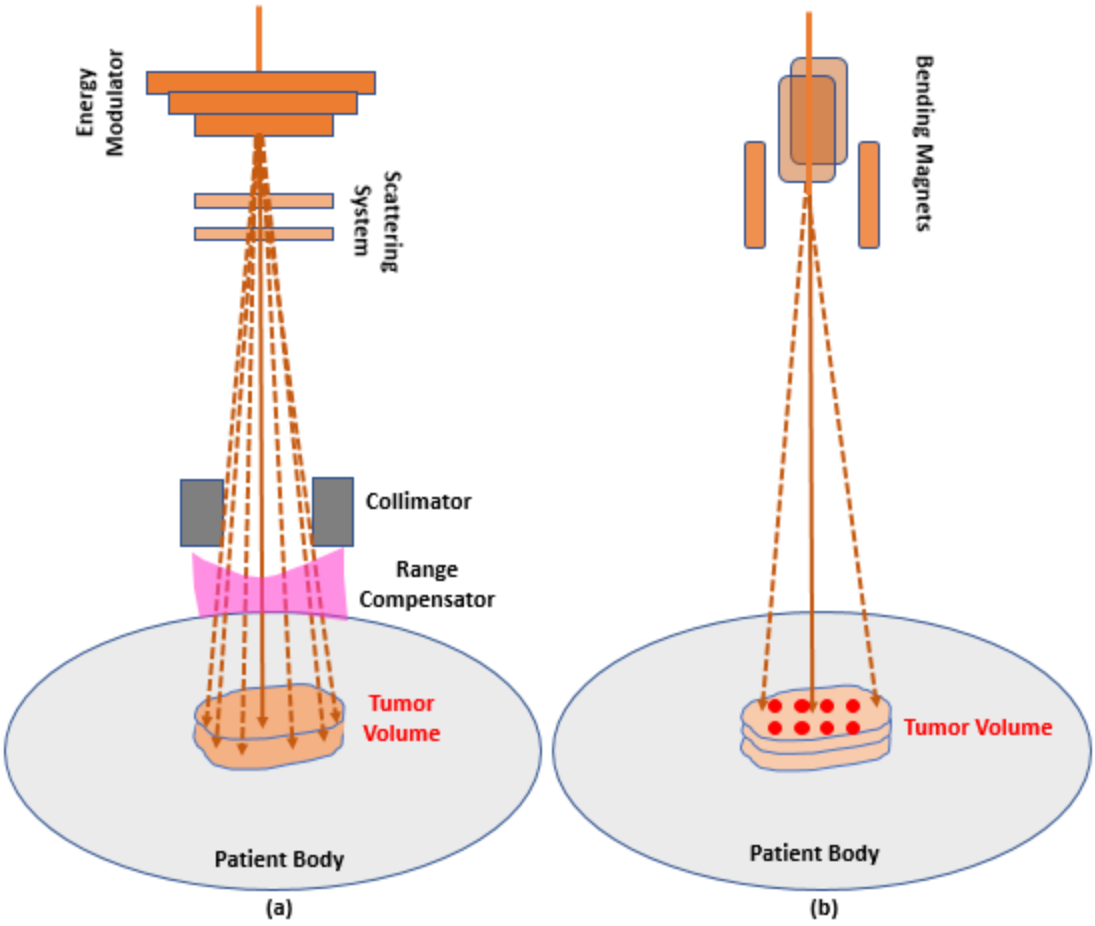

Figure 1.5: (a) Schematic of passive scattering proton therapy and (b) pencil beam scanning proton therapy

1.4.1 Passive Scattering Proton Therapy

In case of passive scattering, materials with high values of atomic number are inserted in the path of the beam in the required dimensions. For the smaller fields, a single scattering material is used in the path of the proton beam to broaden the pencil beam coming out of the accelerator nozzle. For larger fields, a second scattering material is added in the path of the pencil beam to obtain a uniform dose to the target as shown in Figure 1.5-a schematically [4, 7, 17]. This technique of

spreading proton beam over the tumor volume is called passive scattering and the systems having such designs are called double scattering systems for proton therapy.

1.4.2 Pencil Beam Scanning (PBS) Proton Therapy

In case of pencil beam scanning (Figure 1.5-b), the dose distribution shaping is performed with the help of magnetically scanned small gaussian-shaped proton pencil beams (spots). The scanning is performed with the help of fast magnets also called sweepers, which can deflect the pencil beam in two orthogonal planes [7, 18]. This technique functions in such a way that these spots are allowed to fall on a particular location in the target plane. Conventionally, the location is defined in terms of regular rectilinear/hexagonal grids (Figure 1.6 a).

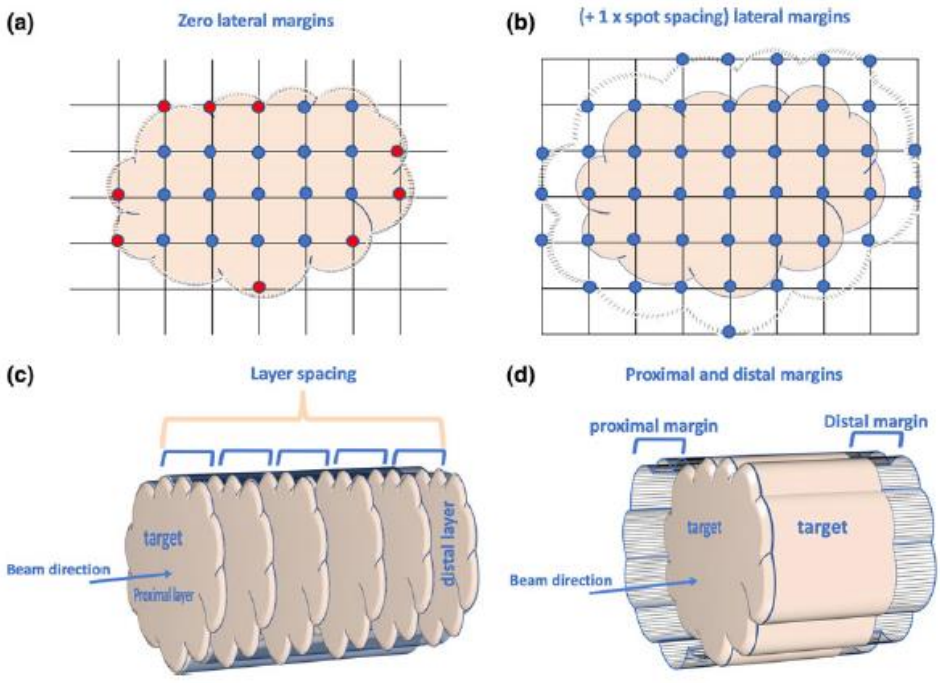

Figure 1.6: Spot placement and energy layer spacing in PBS proton therapy [18]

After irradiating one location, the beam is turned off and the magnet moves this beam to the other location, and it irradiates that location. In doing so, the whole layer of the target is irradiated. The target layer is given a certain margin for the proper coverage of the target edges, typically the margin is set to have one spot outside of the target (Figure 1.6-b). The energy switching system, brings the energy to a lower level and the second layer of the target is irradiated and, in this manner, the whole three-dimensional volume of the target tumor is irradiated (Figure 1.6-c). The nominal energy range of the proton beams in case of pencil beam scanning proton therapy ranges from 70 MeV to 220 MeV and in some cases, it can go up to 250 MeV [18].

CHAPTER 2: TREATMENT PLANNING PARAMETERS IN PROTON PENCIL BEAM SCANNING

Relatively less entrance dose, uniform coverage of the tumor, and rapid dose falloff in both lateral and distal directions are the main dosimetric gains of pencil beam scanning (PBS) proton therapy over other radiotherapy techniques using [4, 19, 20]. These properties allow the proton beams to treat a wide variety of complex-shaped tumors at different anatomical locations while providing superior sparing of normal tissue and organs at risk (OARs) surrounding the tumor.

2.1 Proton Pencil Beam Behavior in Water

When proton beam passes through a medium (water), the dosimetry of the beam depends on various parameters. There are two basic parameters of the scanned proton beam dosimetry (i) range of single pencil beam in water that is determined by the kinetic energy of the protons in MeV and the shape of the dose spots. The shape of the dose spot is characterized by the lateral spot size (perpendicular to the beam direction) at the depth of the maximum dose d_{max} and the longitudinal spot size (along the beam direction) between the proximal and the distal 80% dose location (as well as the proximal and distal 90% dose locations). All these parameters vary with the beam's energy. These parameters are the basic building blocks of any desired dose distribution, and they determine the slope of the dose falloff in the penumbral regions[20]. In addition to these, spot size, inter-spot distance (spot spacing), Bragg peak (spot) placement and number of Bragg peaks (spots) also potentially impact the overall treatment plan quality and treatment time [18, 21-26].

2.2 Parameters affecting treatment plan quality

2.2.1 Spot Size

It has been shown in literature that the smaller spot sizes allow for sharper dose gradients and hence decreased dose to the organs at risk (OARs) [18, 23, 26, 27]. In treatment planning systems (TPS), the beam spot size is defined as a single or double 2D Gaussian function, characterized by its full width at half maximum (FWHM). The spot size is expressed in terms of beam sigma (σ) and is defined in-air at iso-center for a particular energy. The spot sigma is associated with the FWHM by the following equation:

$$FWHM = 2.355\,\sigma$$

In practice, small spot sizes may not be advantageous when dealing with larger tumor volumes because of the unacceptably larger number of spots and increased treatment time.

2.2.2 Spot Spacing

Inter-spot spot spacing is another parameter that has impact on the treatment plan quality, and it shows the distance between the centers of the adjacent spots in one particular energy layer. It is either fixed or can be modified by the user. The spot spacing used in ASTROID treatment planning system was set to be 85% of the effective spot size that is spot sigma at that particular depth. Different treatment planning systems define spot spacing differently and it is critical for reducing the dose ripples across a given energy layer as a function of depth [18]. The spot spacing in the depth direction is defined by the energy switching system and it is also different for different treatment planning systems.

2.2.3 Spot Placement

Spot placement is one of the important treatment planning parameters that has impact on treatment plan quality. In this case, spots (Bragg peaks) are distributed on a regular rectilinear/hexagonal starting grid that is orthogonal to the direction of the incident beam as shown in Figure 1.6 b. The grid points are separated by a distance equal to the spot spacing that is defined differently in different treatment planning systems.

2.3 Proton Pencil Beam Behavior in Water

These treatment planning parameters are dependent on each other and also on the energy of the beam. In a medium of interest (human tissue or water), at low energies, the proton beams exhibit less range straggling, and hence the Bragg peaks are relatively narrow, which means that more beam energies are needed to cover a given target volume at shallow depths, when compared with high-energy beams for deeper target volumes of similar sizes [20]. The behavior of a proton pencil beam in a medium of interest (water) is shown in Figure 2.1 for different proton energies. The beam has been created using ASTROID treatment planning system having an in-air spot size of 4.3 mm at iso-center for 145 MeV energy. Different energy beams are shown in this figure starting from 100 MeV to 200 MeV with a difference of 20 MeV in a water phantom.

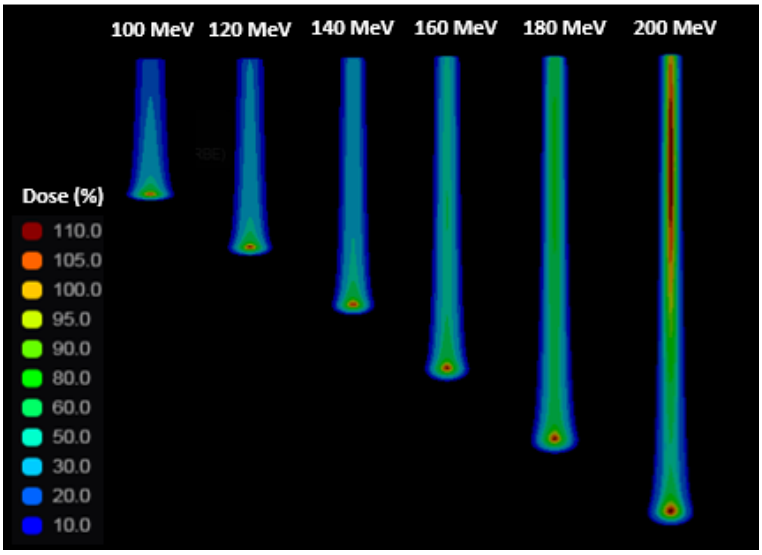

Figure 2.1: Single proton pencil beam in water created using ASTROID treatment planning system for different energies

Similarly, the central axis depth dose profiles for these energies are shown in Figure 2.2. Effective spot size was computed for each of these pencil beams at the iso-center plane and plotted in Figure 2.3 (red line) along with in-air spot size (blue line) for these energies.

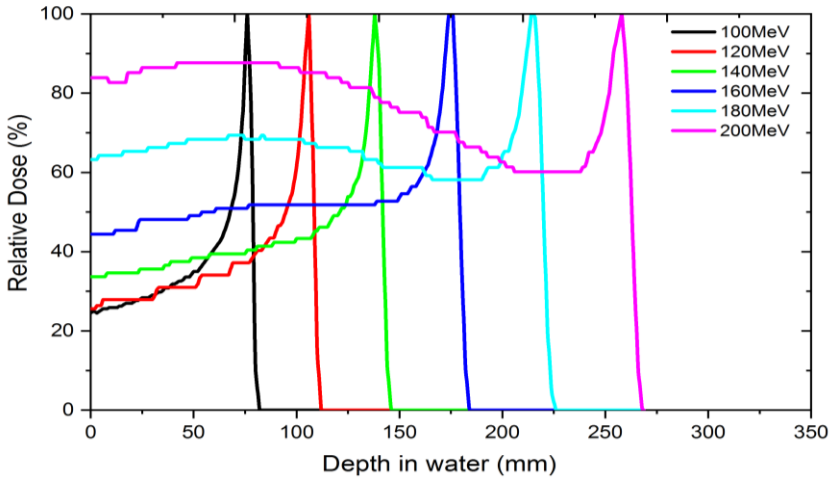

Figure 2.2: Central axis normalized depth dose profiles of single proton pencil beams of energies from 100 MeV to 200 MeV in intervals of 20 MeV in water

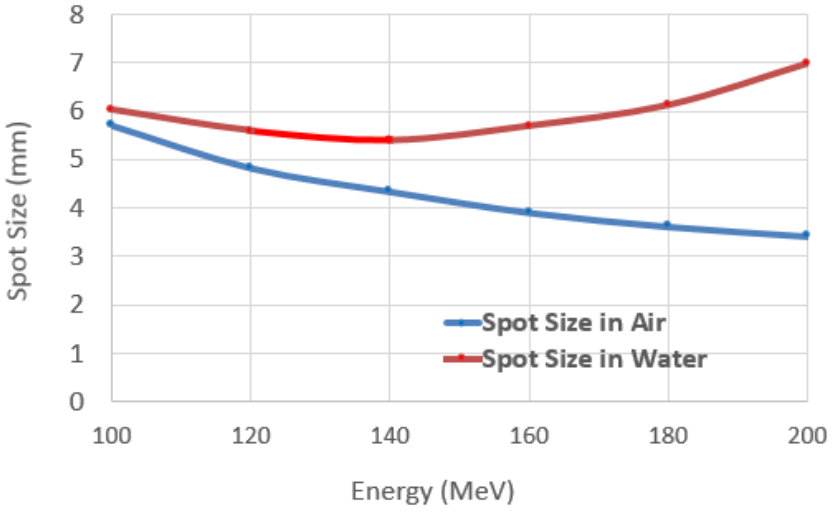

Figure 2.3: Change in spot size of a single proton pencil beam in water and in-air

There is always a change in the actual spot size (in-air) and the spot size at the depth in water due to proton interactions with the medium. The changes in the spot size inside the medium has an important connection with the pre-defined treatment planning parameters; spot placement and spot spacing and affect the treatment plan quality. Since the spot placement is defined considering the in-air spot size, the spot placement may not be similar at a certain depth inside the target phantom for the real 3D patients. Similarly, the pre-selected value of spot spacing would not be the same for spot distribution and hence it will affect the treatment plan quality. However, little attention has been given to spot placement algorithms and the effect of spot placements on target dose coverage and overall plan quality is still a work-in-progress. It is the purpose of this study to shed more light on this important aspect of proton pencil beam delivery.

2.4 Spot Placement in Commercially Available TPS

In commercially available treatment planning systems, spots are calculated and selected on a regular (rectilinear or hexagonal) starting grid. The grid can be a 2D or 3D grid depending upon the vendor. Eclipse (Varian Medical Systems, Palo Alto, CA) uses a 3D grid with adjacent layers of spots aligned and a fixed spot spacing for all energy layers [18, 28]. Pinnacle (Philips Medical Systems) uses a 2D grid for each energy layer with adjacent layers of spots off-set by half the spot spacing. RayStation (RaySearch Laboratories, Stockholm, Sweden) and XiO (Elekta Solutions AB, Stockholm, Sweden) can use either 3D or 2D grids depending on the use of fixed or variable spot spacing [28-32]. The grids defined for spot placement are orthogonal to the direction of the incident proton beam. As the spots are distributed on such grids, to cover the selected target volume completely, spots up to the inter-spot distance outside of the selected target volume must be selected to ensure full target coverage. Failure to select these external spots results in dose under-coverage of the target. The same is true when using a hexagonal grid for the spot placement [7]. This led to the idea of proposing alternative spot placement techniques that selectively place spots directly on the boundary of the target and then fill-in the spots internally as required depending upon the shape of the target for each layer. These techniques have been previously reported as concentric-contours, hybrid, and optimized, and have shown improvement in the treatment plan quality in terms of the dose falloff, reduced number of spots, and more efficient delivery [7, 19, 22, 25].

Therefore, the purpose of this work is to propose an alternative way of spot placement so that improved dose distributions in patients may be achieved. The scope of this work can be divided into two major projects.

Project 1: Development of a new optimized spot placement technique that provides both boundary conformity and inter-spot distance uniformity.

Project 2: Implementation of the newly developed spot placement technique in ASTROID treatment planning system and a dosimetric evaluation of this new technique relative to other available spot placement techniques.

CHAPTER 3: AN OPTIMIZED APPROACH FOR SPOT PLACEMENT

The contents of this section have been published in: ur Rehman, Mahboob, Kevin Erhart, Jerrold Kielbasa, Sanford L. Meeks, Zhiqiu Li, Twyla Willoughby, Naren Ramakrishna et al. "An optimized approach for robust spot placement in proton pencil beam scanning. "Physics in Medicine & Biology 64, no. 23 (2019): 235016.

3.1 Introduction

Pencil beam scanning (PBS) proton therapy is an advanced form of proton therapy delivery that has revolutionized the practice of particle therapy in recent years [4, 33]. In PBS treatments, a narrow beam of protons is magnetically steered in the plane transverse to the incident beam direction, allowing for the creation of complex field shapes without the need for patient-specific hardware or multi-leaf collimators (MLCs) [7, 19]. Since the pencil beam locations can be precisely controlled, proton PBS offers a flexibility in shaping the dose distribution delivered to a patient that is superior compared to other existing proton and conventional radiotherapy techniques. The planning of proton PBS treatments typically involves determining the maximum and minimum proton energies needed to cover the target, splitting this range of energies into a finite number of available energies (layers), and then distributing a regular grid of pencil beam delivery locations (spots) to the target in a 2D layer-by-layer fashion. Field shaping and treatment optimization are then performed by determining the optimal proton fluence to deliver for each of these fixed spots in order to achieve a highly conformal dose distribution [34, 35].

Commercially available treatment planning systems (TPS) such as Varian Eclipse (Varian Medical Systems, Palo Alto, California), and RayStation (RS; RaySearch Americas, Garden City, New

York) employ fixed spot placement techniques based on rectilinear and hexagonal grids orthogonal to the direction of incident field to define the spot positions that will be delivered to the patient from each energy layer for each user selected field direction. With such grid-based techniques, spots with centers outside of the tumor boundary must be included in some areas in order to provide full dose to the target at the edges. This results in sub-optimal conformality, slow dose falloff, and may not provide desirable integral dose outside of the target, especially near critical OARs. The spatial positions of the individual proton pencil beams are generally pre-defined and fixed, as their inclusion within plan optimization significantly increases the complexity of the optimization process. While the current fixed spot PBS techniques do reduce the computational burden and eliminate the need for patient-specific beam shaping devices, this comes at the expense of an increased lateral dose falloff (penumbra) compared to more traditional passively scattered proton therapy treatments [19]. So, while grid-based spot placement techniques may be simple to implement and use, they do not allow clinicians to take full advantage of the delivery capability of today's advanced proton PBS systems.

Achieving a sharp lateral dose falloff is of primary interest in proton PBS as this is crucial for sparing organs at risk (OARs), especially when they are in close proximity to the target. A few approaches have been proposed to improve lateral dose falloff, such as use of solid brass apertures and movable collimators (dynamic collimation system (DCS) and Mevion's Adaptive Aperture (Mevion Medical Systems Inc., Littleton, MA)) , spot size reduction and using improved scanning pattern of pencil beams (spot placement) [19, 23, 27, 36, 37]. Movable collimation systems have proven feasible but come at the cost of prolonged treatment time due to the mechanical movement of collimators, increased cost, and compatibility issues for existing PBS systems. In addition, an

increased secondary neutron dose has also been reported when using these kind of movable collimator systems [17]. Spot size reduction has shown gains in treatment plan quality by improving the lateral penumbra. Clinically available spot sizes vary significantly ranging from 3 mm to 15 mm, with only a few of the existing delivery systems having the capability to produce a spot size small enough to achieve an improved lateral dose fall-off and plan quality compared to other radiotherapy techniques [34, 38, 39]. Since spot size is a machine dependent parameter and is fixed with the machine design, reducing the spot size in existing systems is generally not a viable option for existing facilities.

Recently, advanced placement of spots in the lateral direction has been investigated as an alternative means to provide improved treatment plan quality by reducing lateral penumbra. These spot placement techniques include concentric-contours and hybrid scanning approaches [7, 19, 22]. Such research has shown that improved spot placement techniques can sharpen the lateral dose falloff, thereby increasing the dose conformity. And most importantly, most current proton delivery systems already support arbitrarily complex spot placements, making this approach an attractive, accessible, low-cost option to improve proton PBS plan quality. Additionally, other investigations have shown that improved spot placement techniques can also enhance the effects of collimation, providing further benefit even for machines with advanced moveable collimation systems [40].

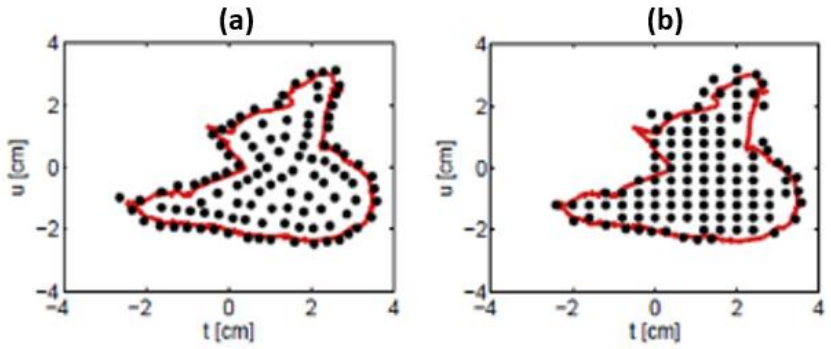

Figure 3.1: Concentric contours and hybrid spot placement techniques [22]

Although, the contour-based spot placement scheme (Figure 3.1-a) improves the boundary conformity by maintaining all spots within (or a fixed distance beyond) the tumor boundary, these benefits come at the expense of maintaining uniformity of spot distribution inside the target volume. Past works did include a hybrid scheme that attempts to address this concern, but the hybrid approach suffers from having the non-uniformity region close to the tumor boundary (Figure 3.1-b); a sub-optimal location, as the goal is to fully exploit the benefits of edge enhancement [22]. Therefore, an alternative spot placement scheme is desired that can achieve the boundary conformity of a contoured approach and a seamless transition to a uniform distribution of interior spots as is found in rectilinear/hexagonal grids. The development of such an approach is the focus of this work.

3.2 Methods and Materials

This work breaks away from traditional grid-based and geometry aligned spot placements and introduces a process to create optimized distributions of spots within a target. The objective is to develop an optimized spot placement scheme to achieve boundary conformity, as in the case of

contour-based techniques (concentric-contours and hybrid), and internal spot uniformity, as in the case of grid-based techniques. In addition to describing the new optimized spot placement scheme, this work also provides a comparative study of existing spot placement techniques and highlights the key features of the various techniques and their effect on treatment plan quality.

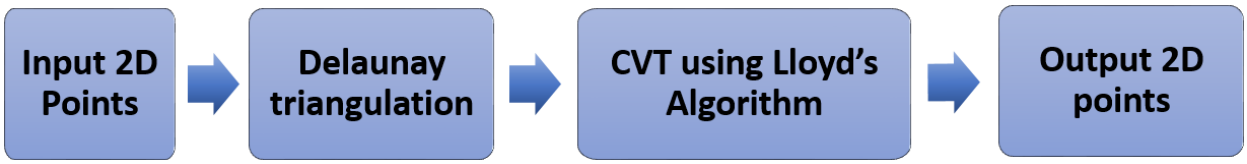

Figure 3.2: The algorithm to develop optimized spot placement scheme using Delaunay

Figure 3.2 shows the algorithm for developing our optimized spot placement scheme in which an input set of spot locations from a modified hybrid scheme (a single row of boundary contoured spots with the interior filled with a hexagonal, instead of rectilinear, grid of spots) is used as the starting point. An iterative approach using a Delaunay triangulation of spot centers followed by Centroidal Voronoi Tessellation (CVT) has been developed to create a highly uniform, but boundary conforming distribution of spots. MATLAB (MathWorks, Inc.) was used to develop the code for the optimized spot placement scheme. To test this scheme, two target shapes were created having a convex and concave geometry as shown in Figure 3.3.

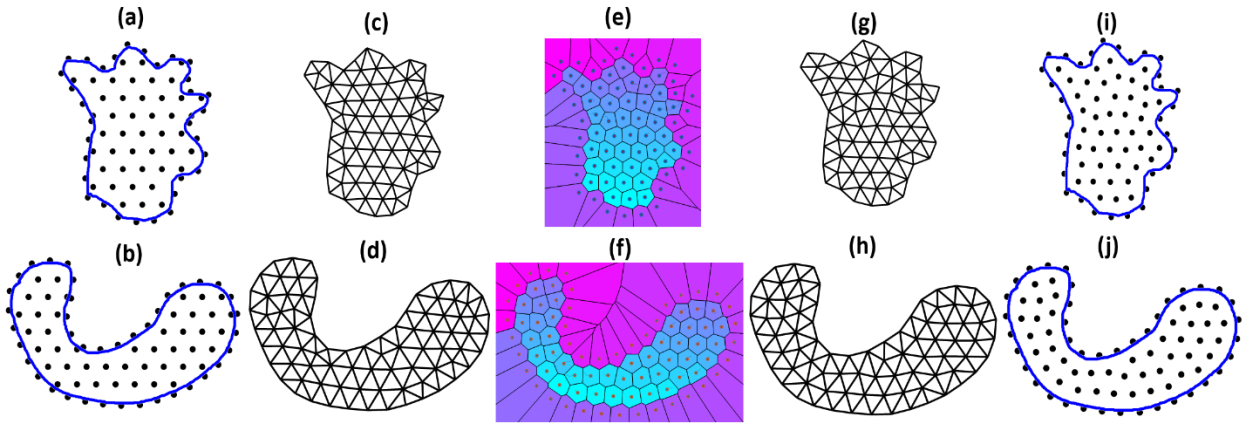

Figure 3.3: Optimized spot placement scheme for convex and concave target shapes. Input set of 2D points (a-b), initial triangulation (c-d), CVT using Lloyd's algorithm (e-f), final triangulation (g-h), output 2D points (i-j)

The input set of points was taken from hybrid spot placement scheme by replacing the rectilinear grid used in hybrid by a hexagonal one as shown in Figure 3.3-(a-b) and a Delaunay triangulation was performed to connect the centers of these spots. This created an initial triangular mesh in the target plane as shown in Figure 3.3-(c-d) that provided appropriate connectivity of spots to allow for measurement of spot placement uniformity as the variance of the edge lengths in the Delaunay triangulation. After Delaunay triangulation, CVT was performed on these points using Lloyd's algorithm [41, 42]. In Lloyd's algorithm, for a given collection C of points in a region, the Voronoi diagrams are obtained which break the region into cells in such a way that the cell for a point z in C consists of all points in the region closer to z than to any other point of C. The Voronoi patches are shown in Figure 3.3-(e-f) for convex and concave shapes respectively. After computing the Voronoi diagrams, the points in C are moved to the centroids of the current Voronoi patches. This process continues iteratively so that in the final Voronoi diagram, each point in C coincides with

the centroid of its Voronoi patch. As the aim was to maintain boundary conformity in our spot distribution, the restriction of fixing the boundary points and allowing only the interior spots to move was imposed. After few iterations, the mesh points are uniformly distributed in the region in an optimal way and the distribution pattern is a smooth progression from boundary conformal to a hexagonal interior distribution as shown in Figure 3.3-(g-j).

3.2.1 Geometrical Validation

The optimized spot placement scheme was validated geometrically by designing a square target as a test case. The ideal spot distribution for optimal target coverage is shown in Figure 3.4-a. The central spot was then perturbed to get a non-uniform spot distribution (Figure 3.4-b). The optimized spot placement algorithm was then applied to this non-uniform distribution (Figure 2.4-c). After a few CVT iterations, the ideal position for the central spot was reached as shown in Figure 3.4-(c-h).

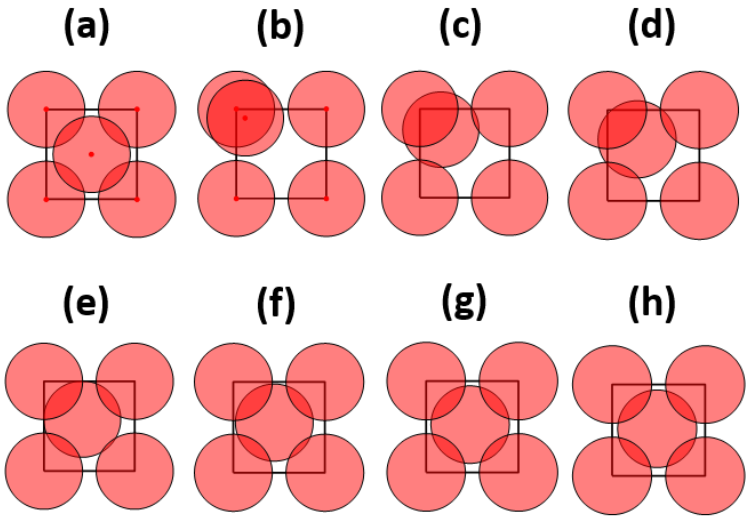

Figure 3.4: Geometric Validation of the optimized spot placement scheme

3.2.2 Geometrical Representation

The spot placement have been defined as geometrically optimal due to the fact that it minimizes the variance of spot center-to-center distances (edge lengths in the Delauney triangulation) within the target volume ($D_{Variance}$) while maintaining target boundary conformality. Using the convex and concave target shapes, several key metrics have been quantified that demonstrate the optimal nature of this new approach as compared to other spot placement techniques. $D_{Variance}$ was computed as follows:

$$D_{variance} = \frac{1}{N-1} \sum_{i=1}^{N} | x_i - \mu |^2$$

where x_i is the length of the i^{th} edge, μ is the mean of the triangle edge lengths, and N is the total number of edges in the triangulation formed by joining the spot centers. According to this metric, a hexagonal spot distribution is ideal, as it produces a uniform, equilateral triangulation, resulting in $D_{Variance} = 0$. This demonstrates that $D_{Variance}$ is a simple, straightforward optimization metric for uniformity, as smaller values are more desirable.

3.3 Treatment Planning Study

While geometric optimality is the major objective in this work, it is not the only metric of significant importance. As such, our new optimized spot placement scheme was implemented in the commercial ASTROID (:decimal LLC) treatment planning system in order to investigate the potential of the optimized spot placement scheme for realistic targets, as compared to the other existing commercial and research techniques described above. The two test cases used above were extended to 3D and placed within a water phantom to create two simulated patient targets having

convex and concave geometries matching those used in Figure 3.3. The concave shape target was simulated as wrapping an OAR while the convex shape target has a very irregular. As the focus in the initial phase of this research has been on optimal in-plane (2D) spot distributions, these targets were designed to be planar, therefore, thickness of the targets was kept small (~6 mm) making the targets thin slabs so that three-dimensional effects could be minimized (toward this end, five energy layers (155 MeV to 147 MeV) were used with identical spot placements to ensure a uniform dose distribution in the beam axis direction). The maximum dimensions were 140 mm and 100 mm for the concave shape and the convex shape targets, respectively, to simulate realistic clinical target sizes. A spot size having in-air sigma of 12 mm was used for all spot placement techniques, which is in the mid- to high-range of typical PBS spot sizes for active proton centers at the moderate energies (145 MeV) used herein. To ensure that there are no optimizer-based dependencies for implementation of each spot placement techniques, A set of fixed optimizer controls in combination with DVH-based constraints was specified for each scheme as follows.

Constraints:

100% of the tumor volume must receive 98% dose

Maximum dose must be less than 120% of Rx dose

Objectives:

Normal tissue dose was minimized by maximizing conformality index

In the case with adjacent OAR, maximum and mean dose to the OAR were both minimized. As ASTROID includes an advanced Multi-Criteria Optimizer, various TPS objectives and optimizer controls were used to drive these stated objectives to the best possible values while not violating

the two constraints listed above. Dose covering 95% of the target volume (D95), Integral Dose (ID) to the normal tissue, Lateral dose falloff (Penumbra), Homogeneity index (HI) and conformity index (CI) were computed for both targets to allow for comparison of the dosimetric performance of each spot placement scheme.

3.4 Results

Our results quantify the differences of our new optimized spot placement scheme through direct comparison with grid-based and contour-based spot placement techniques. The spatial distribution of spots, planar dose distributions, as well as several key metrics are presented for various spot placement techniques and compared for two target shapes.

3.4.1 Spatial Distribution of Spots

The spatial distribution of spots in the test target shapes is shown in Figure 3.5 for all spot placement techniques. The spots were represented by red circles with a slight transparency level to help highlight the areas of spot overlap (circles are sized at the in-air spot sigma at isocenter). The target boundary is represented by the black line and a hypothetical OAR in the form of a circle is shown within the concavity of the concave shape target to simulate realistic clinical situations.

Figures 3.5(a-b) and (c-d) show the spot distributions using grid-based (rectilinear/hexagonal) techniques. In both techniques, it can be seen that some spots outside of the target boundary must be included in order to have complete coverage of the target. If these spots are not selected, the target can be under-dosed, whereas if these spots are selected, it can give increased dose outside of the target boundary. This may also lead to extra dose in the adjacent OAR due to these

extraneous spots. Figure 3.5(e-h) show how contour-based and hybrid techniques place spots along the boundary in a more conformal way, but this comformality comes at the expense of non-uniform spot distributions inside the target, either at the core (contour) or the contour-grid interface region (hybrid). Figures 3.5(e-h) also provide a geometrical validation of the work performed by Paul Scherrer Institut [22]. Our proposed optimized spot placement scheme (Figure 3.5(i-j)) provides a high-quality distribution of spots in terms of boundary conformity and uniformity inside the target area. It is clear from these cases that this approach achieves the conformality of the contoured techniques and the internal uniformity of grid techniques, with a smooth, gradual transition between the two in the near-boundary region.

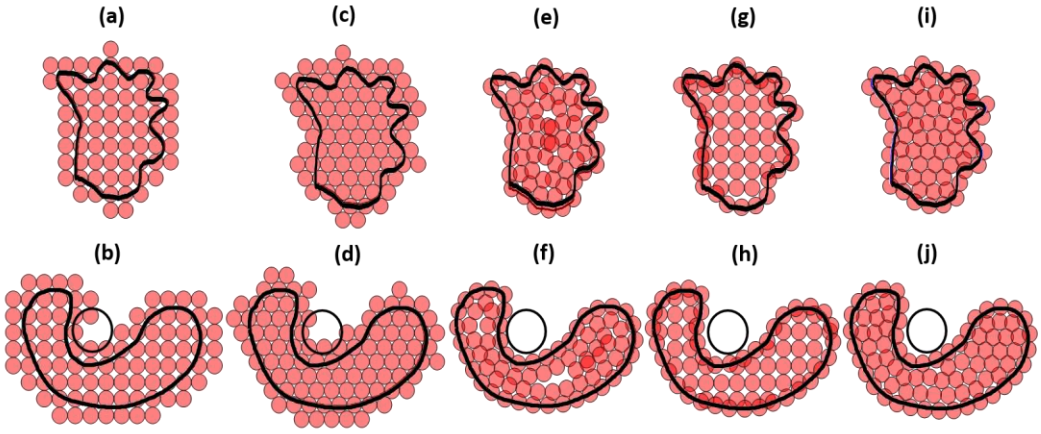

Figure 3.5: Geometrical representation of spot distribution using rectilinear grid (a-b), hexagonal grid (c-d)m contours (e-f), hybrid (g-h) and optimized (i-j) spot placement techniques

This qualitative view proved promising; however, a more objective quantification is necessary to remove bias. As described above, the variance of spot center distances is an appropriate measure of uniformity of a spot distribution.

Table 3.1: Variance in inter-spot distance for different spot placement techniques

Spot Placement Techniques	**$D_{Variance}$ (Convex)**	**$D_{Variance}$ (Concave)**
Rectilinear Grid	61.3	62.1
Hexagonal Grid	0.0	0.0
Concentric Contours	100.8	78.2
Hybrid	89.0	103.1
Optimized	16.6	15.5

This variance data has been computed for each case in Figure 3.5 and is provided in Table 3.1. The hexagonal grid-based distribution has a zero $D_{Variance}$ as it is a completely uniform spatial distribution. This zero-variance value can be considered as the reference value because the ideal spatial distribution is hexagonal distribution and other techniques should be compared with respect to this value in terms of uniformity. The optimized spot placement technique gives a clear advantage in uniformity as these variance values for both convex (16.6) and concave (15.54) shape targets are significantly reduced as compared with the remaining spot placement techniques tested herein.

3.4.2 Planar Dose Distribution

Planar slice views (perpendicular to the incident beam direction) of the resulting dose generated using all available spot placement techniques are shown in Figure 3.6(a-j) for both convex and concave targets. In each case, the dose was optimized to improve the conformity, but in the case of the concave shape target, a dose objective was also set to spare the nearby OAR as much as

possible. The calculated dose distributions show a clear reduction of dose in the surrounding area of the target in both concave and convex shape targets (Figure 3.6(a-j)) when using contour, hybrid, and optimized spot placement techniques as compared to the traditional grid-based spot placement techniques. Qualitatively, Figures 3.6(a-d) show that grid-based techniques provide excellent dose uniformity, but slightly less conformality. Using the evaluation metrics, these differences were quantified in Tables 3.2 and 3.3.

Lateral dose profiles for convex and concave shape targets are shown in Figure 3.7(a-b), taken at the locations highlighted by white lines in Figure 3.6(a-b). The profiles are important analysis tools since they show that the proposed optimized spot placement technique has achieved not only a slight decrease in lateral penumbra, $P_{80\text{-}20}$, but also improved conformality, as it can be seen the location of the 95% dose is much closer to the target edge for the contour, hybrid, and optimized techniques (highlighted by the arrow in Figure 3.7-b. The dose volume histogram analysis of the target, OAR and normal tissue is shown in Figure 3.8 (a & b) for both convex and concave shape targets.

3.5 Discussion

In this work, a new method of spot placement in PBS proton therapy have been proposed and tested which distributes spots inside the target plane in a geometrically optimal fashion in an attempt to improve lateral dose conformity while maintaining target dose uniformity. In this approach, the target boundary is first covered by spots equidistant from each other along the boundary contour and the target area is then filled in such a way that the final spot distribution transitions smoothly from boundary aligned to a nearly hexagonal distribution (Figure 3.6-(i-j)).

To achieve this optimal spot distribution, an iterative technique using Delaunay triangulation and Central Voronoi tessellation (CVT) has been used as described herein.

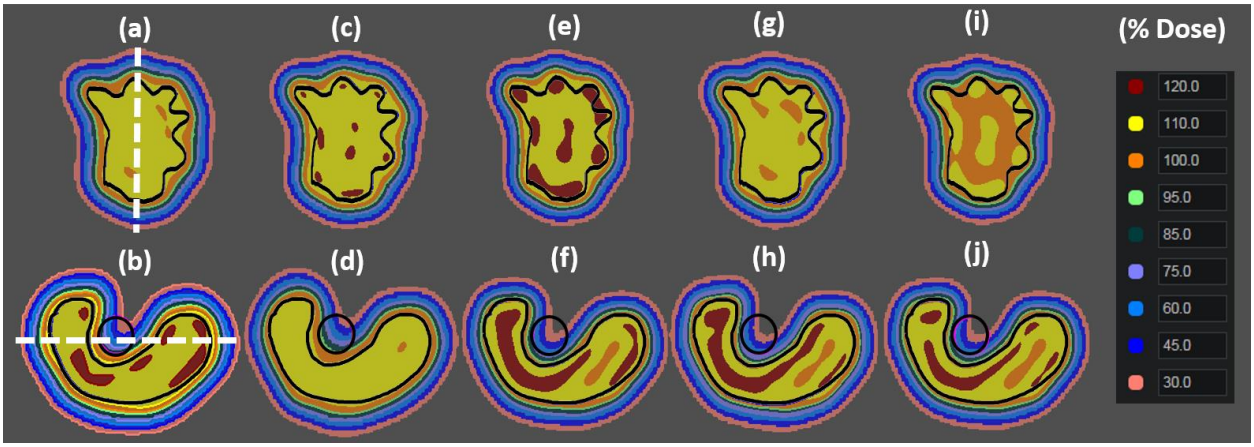

Figure 3.6: Transverse views for concave and convex shape targets using (a-b) rectilinear grid, (c-d) hexagonal grid, (e-f) concentric contours, (g-h) hybrid and (i-j) optimized spot placement techniques.

The spatial (geometric) distribution of spots was evaluated by measuring the variance in the distance between neighboring spot centers and a geometrical validation using two complex target shapes clearly demonstrated the reduction of variance in the new optimized scheme as compared to other existing spot placement techniques; with the optimized scheme out performing all other and approaching the uniformity of the ideal hexagonal grid-based scheme (see Table 3.1). The newly developed spot placement scheme has also been implemented in the commercial treatment planning system ASTROID and feasibility studies were performed using two thin-slab targets having convex and concave geometrical shapes.

This approach was found to be favorable dosimetrically when compared to commercially available grid-based techniques, and comparable to more recently proposed advanced spot placement

techniques (concentric-contours and hybrid) [13]. Figures 3.6, 3.7, & 3.8 highlight the improvement in lateral dose falloff, lateral dose conformity, and normal tissue avoidance that can be achieved with the optimized spot placement scheme and Tables 3.2 (convex) & 3.3 (concave) further summarize these results with quantitative metrics.

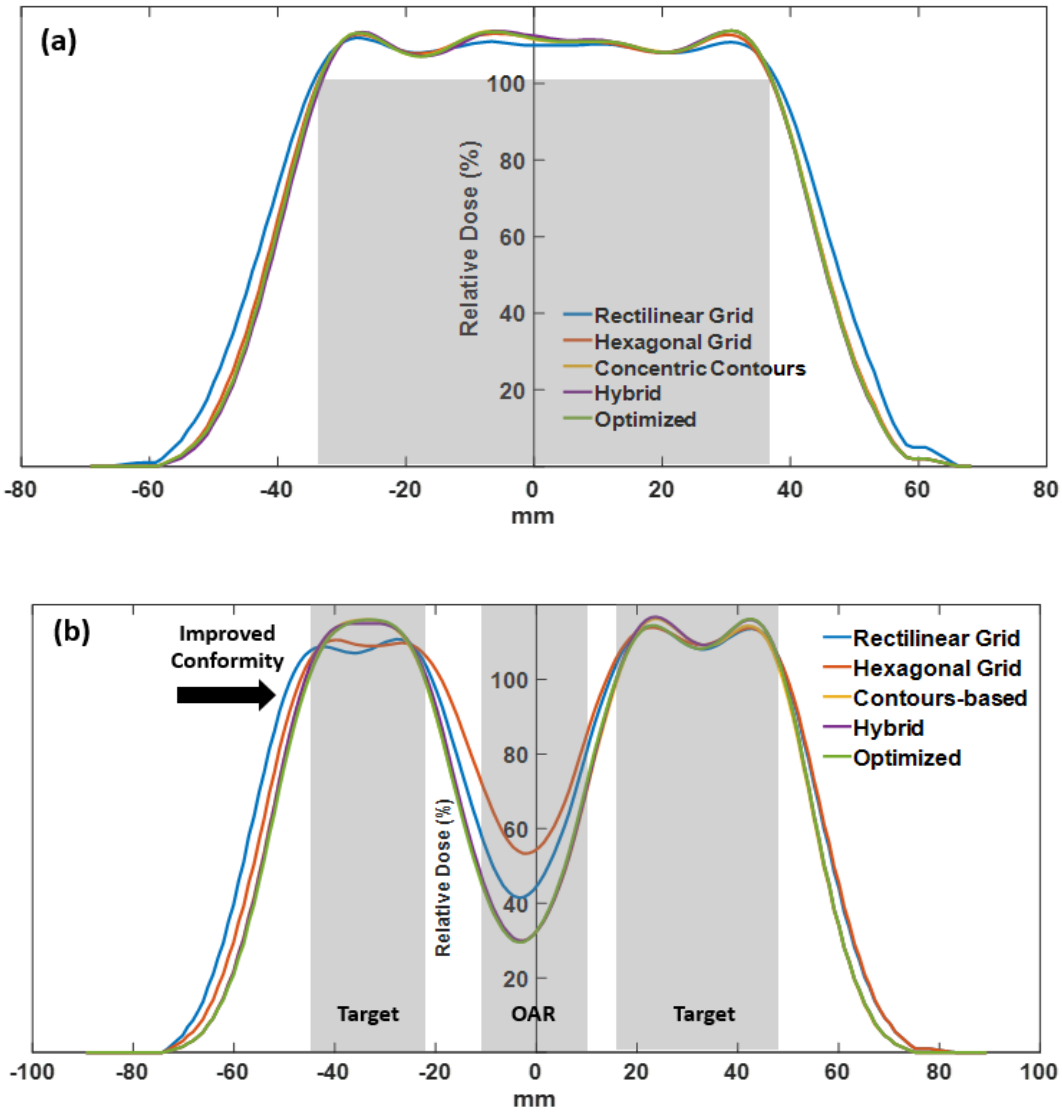

Figure 3.7: Lateral dose profiles (a) Convex shape target, (b) Concave shape target

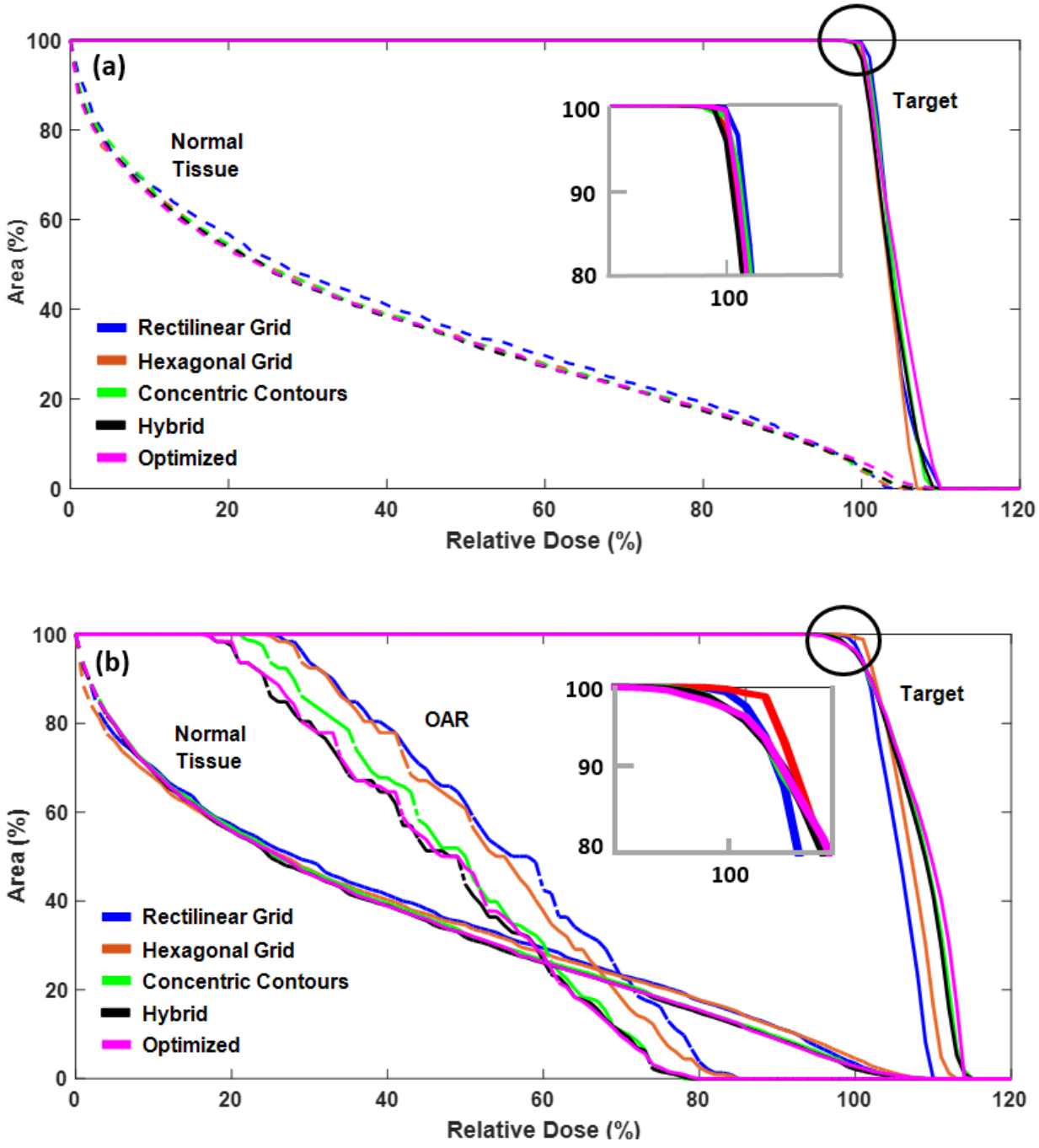

Figure 3.8: Dose Volume Histograms for (a) Convex shape target, (b) for concave shape target

Table 3.2: Dose metrics for convex shape target

Metrics	Rectilinear Grid	Hexagonal Grid	Concentric Contours	Hybrid	Optimized
D_{95} (%)	95.7	94.3	91.3	96.2	98.5
ID (Gy-cm^2)	7.6	6.94	5.96	5.90	6.01
$P_{80\text{-}20}$ (mm)	11.43	11.0	10.3	10.1	9.59
HI (D_{max}/D_{mean})	1.05	1.03	1.04	1.05	1.04
HI (D_{max}/D_{min})	1.12	1.12	1.13	1.14	1.12
CI	1.46	1.44	1.46	1.37	1.35
Spots Count	72	83	78	72	76

Table 3.3: Dose metrics for concave shape target

Metrics	Rectilinear Grid	Hexagonal Grid	Concentric Contours	Hybrid	Optimized
D_{95} (%)	94.1	97.0	96.0	96.1	97.0
OAR D_{mean} (%)	56.2	54.3	49.1	47.3	47.2
ID (Gy-cm^2)	11.19	10.84	7.85	7.71	7.78
$P_{80\text{-}20}$ (mm)	12	11	10.2	9.78	10.0
HI (D_{max}/D_{mean})	1.12	1.14	1.23	1.21	1.22
HI (D_{max}/D_{min})	1.05	1.05	1.06	1.06	1.06
CI	1.47	1.42	1.29	1.27	1.26
Spots Count	85	99	87	84	84

From these results, two important observations can be made, first, grid-based techniques do provide for improved dose uniformity (lower maximum dose values) and second, all of the boundary conformal techniques (contour, hybrid, optimized) seem to provide very similar

dosimetric results. This result is not entirely unexpected, as the goal of improving lateral dose fall off requires the ability to take advantage of the "edge enhancement" effect [19]. This naturally produces an increased dose near the target edge in order to increase the rate of lateral fall-off. It has demonstrated a robust spot distribution inside the target through the proposed optimized spot placement scheme that can provide an attractive, low-cost option to improve proton PBS plan quality.

CHAPTER 4: DOSIMETRIC IMPACT OF USING DIFFERENT SPOT PLACEMENT TECHNIQUES

4.1 Objective

The objective of this part of the work is to study the dosimetric impact of existing spot placement techniques, as well as the newly proposed optimized spot placement technique, on overall treatment plan quality, and to explore the effect of spot size on treatment plan quality in regard to spot placement techniques. In this work, a treatment plan quality comparison for five proton pencil beam spot placement techniques has been performed using ASTROID treatment planning system and using the customized homogeneous phantoms. The impact of these spot placement techniques was studied on treatment plan quality in terms of maximum dose inside the target, dose falloff in both lateral and distal directions, dose uniformity, and dose homogeneity.

4.2 Materials and Methods

We used the ASTROID treatment planning system (.decimal LLC, Sanford, FL) to create two cubical shape homogeneous water phantoms to study the effect of spot placement techniques on the dose distribution and plan quality. The first phantom has a spherical target volume of 50-mm diameter centered at a depth of 75 mm from the surface of the phantom. The second phantom has a conical target volume with a base diameter of 62 mm and height of 60 mm. The base of the cone is placed at a depth of 90 mm from the surface of the phantom as shown in Figure 4.1.

The spherical target volume serves as a useful tool to study the dose falloff in terms of lateral and distal penumbra as well as dose conformity. In this work, we have made use of two distinct spot sizes to provide a realistic analysis based upon the availability of spot sizes in commercially

available proton delivery systems. A medium spot size was used having an in-air sigma of 5.8 mm defined at isocenter for 145 MeV energy. This spot size is in the mid to high range of typical pencil beam scanning spot sizes for active proton therapy centers at moderate energies (~145 MeV). A small spot size was also used to show the impact of smaller spot sizes on spot placement. The small spot size used has an in-air sigma of 4.3 mm at iso-center at 145 MeV energy.

Since the final dose distribution in the target volumes have a strong dependency on the dose optimization in ASTROID, we defined and implemented a set of constraints in combination with DVH-based objectives to provide a fair comparison between the spot placement techniques. The lateral and distal margins for the treatment planning were set at 13 mm and 10 mm, respectively for all spot placement algorithms, while the spot spacing was set to be $0.85\sigma_z$ where σ_z is the spot sigma at the depth z in the beam direction. A uniform calculation grid of 8 mm was defined over the entire patient, and a fine grid of 2 mm was created over the expansion volume of the PTV for both target volumes. This fine grid helps ensure the dose gradients and penumbra region dose is accurately computed. The geometric centroid of both target volumes was selected as isocenter for the beam with an air gap of 50 mm.

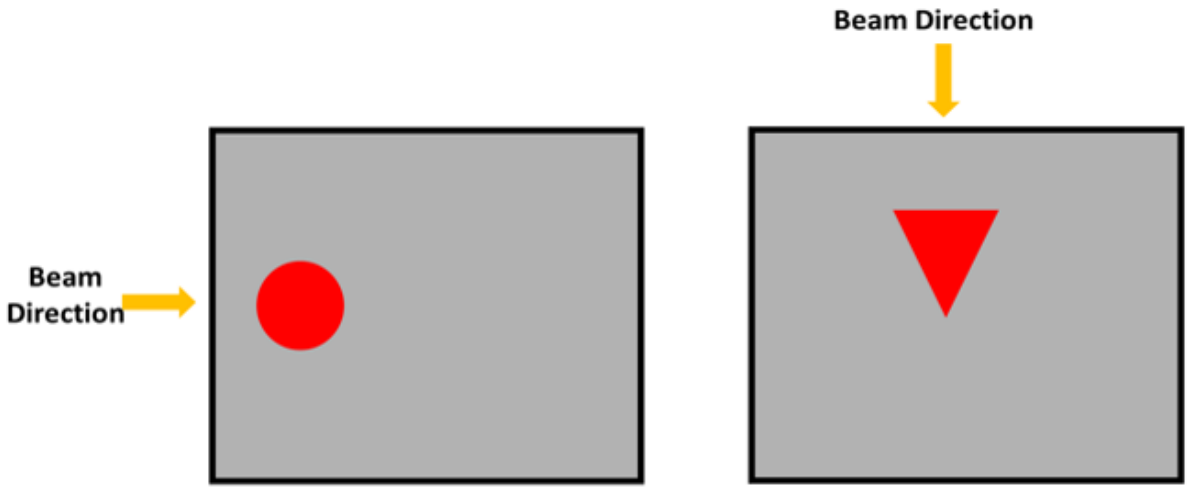

Figure 4.1: Customized homogeneous water phantoms having spherical target volume and conical target volume

Treatment plans were created for each spot placement technique using the ASTROID treatment planning system. To ensure a fair comparison, each plan was constrained to achieve full (100%) coverage of the tumor volume by the Rx dose and a global maximum dose of 112% was allowed. It should be noted that setting a reasonable maximum dose is very important for this study, as it provides each spot placement technique with the same opportunity to take advantage of the edge-enhancement effect previously described by Pedroni et al [19]

ASTROID's advanced Multi-Criteria Optimization (MCO) tool [29, 31, 43] was then configured with several competing objectives designed to allow for efficient exploration of the trade-offs between target coverage, maximum dose, and dose conformality. The MCO controls were used to drive each plan to a dose field that achieved the best possible combination of the metrics identified below while not violating the constraints described above. Lateral and distal dose falloff in terms

of Penumbra (P80-20) was measured and recorded for comparison of each spot placement technique. The following metrics were calculated to evaluate the overall treatment plan quality:

- D_{max}: Maximum dose inside the patient
- P_{20}^{80}: Dose falloff in terms of lateral and distal penumbra
- Conformity Index (CI) and Homogeneity Index (HI)
- Integral dose (ID) to the normal tissue
- Total spot count to achieve same level of meterset weight

4.3 Results

The planned dose distributions for both the spherical and conical target volumes are shown in Figure 4.2 for all spot placement techniques using the medium and small spot sizes. All treatment plans presented here are utilizing single field uniform dose optimization in ASTROID. The advantage of using simple spherical and conical target volumes in a homogeneous medium is that it can highlight the effects of the spot placement techniques that can be masked while using more complex target volumes. Also, as the shortcomings of the grid-based spot placement techniques are evident even in these simple targets it should be clear that they would be even greater in more complex targets and/or when considering heterogeneous media.

Figure 4.2 shows the improved level of dose conformity when using the boundary contoured (concentric-contours, hybrid and optimized) spot placement techniques as compared to the grid-based spot placement techniques. Additionally, the decreased level of dose homogeneity can be seen even in these simple targets when using the boundary contoured spot placement techniques

as compared to the grid-based techniques that can be more prominent in the complex target volumes.

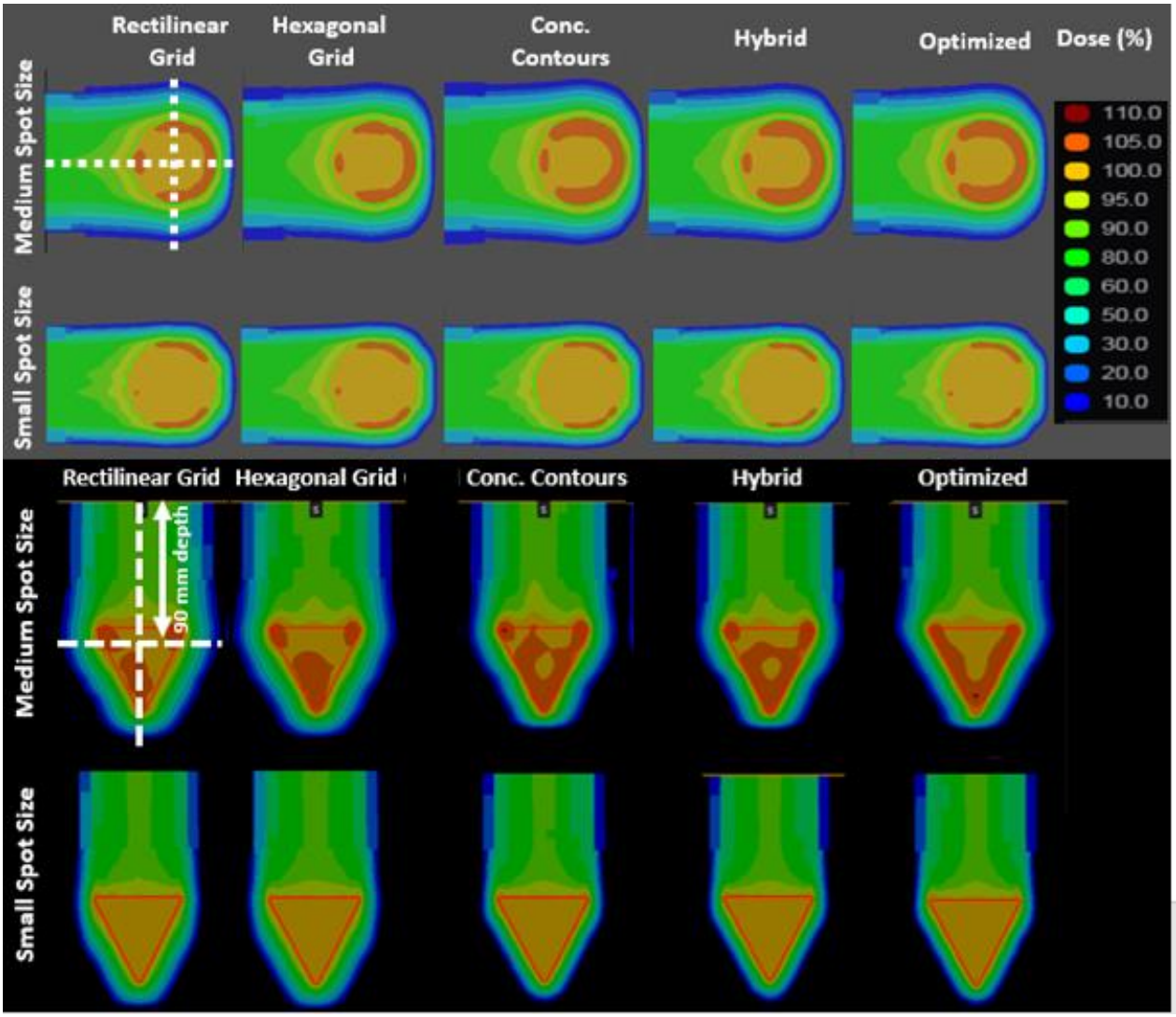

Figure 4.2: Planned dose distributions for spherical target volume using medium spot size (row 1), spherical target volume using small spot size (row 2), conical target volume using medium spot size (row 3), conical target volume using small spot size (row 4) using different spot placement techniques

The lateral and central axis dose profiles for the spherical target volume were obtained at the locations shown in Figure 4.2 by the white dotted line and are shown in Figure 4.3 using medium and small spot size. The profile for the spherical target volume was taken at the depth of 75 mm depth from the surface of the water phantom.

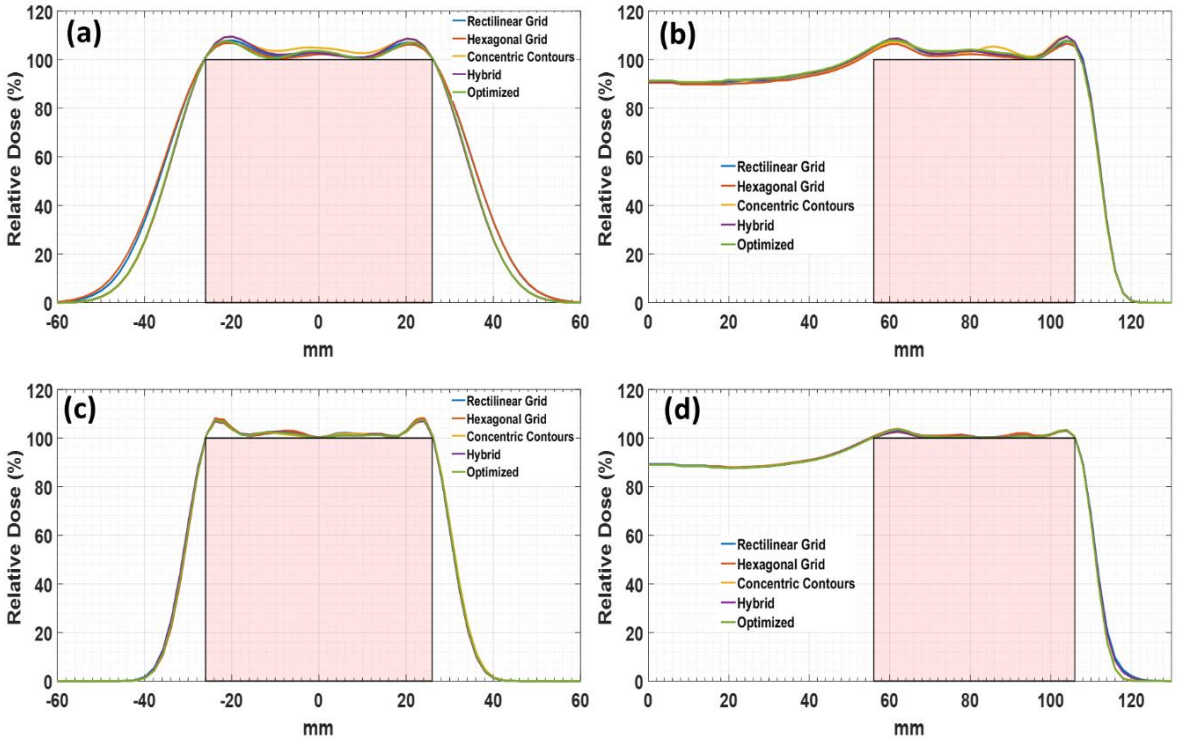

Figure 4.3: Lateral and central axis dose profiles for spherical target volume using medium spot size (row 1), small spot size (row 2) using different spot placement techniques

The lateral and central axis dose profiles for the conical target volumes were obtained at the locations shown in Figure 4.2 by the white dotted line and are shown in Figure 4.4 using the medium and small spot sizes. The profile for the spherical target volume was taken at the depth of 90 mm from the surface of the water phantom.

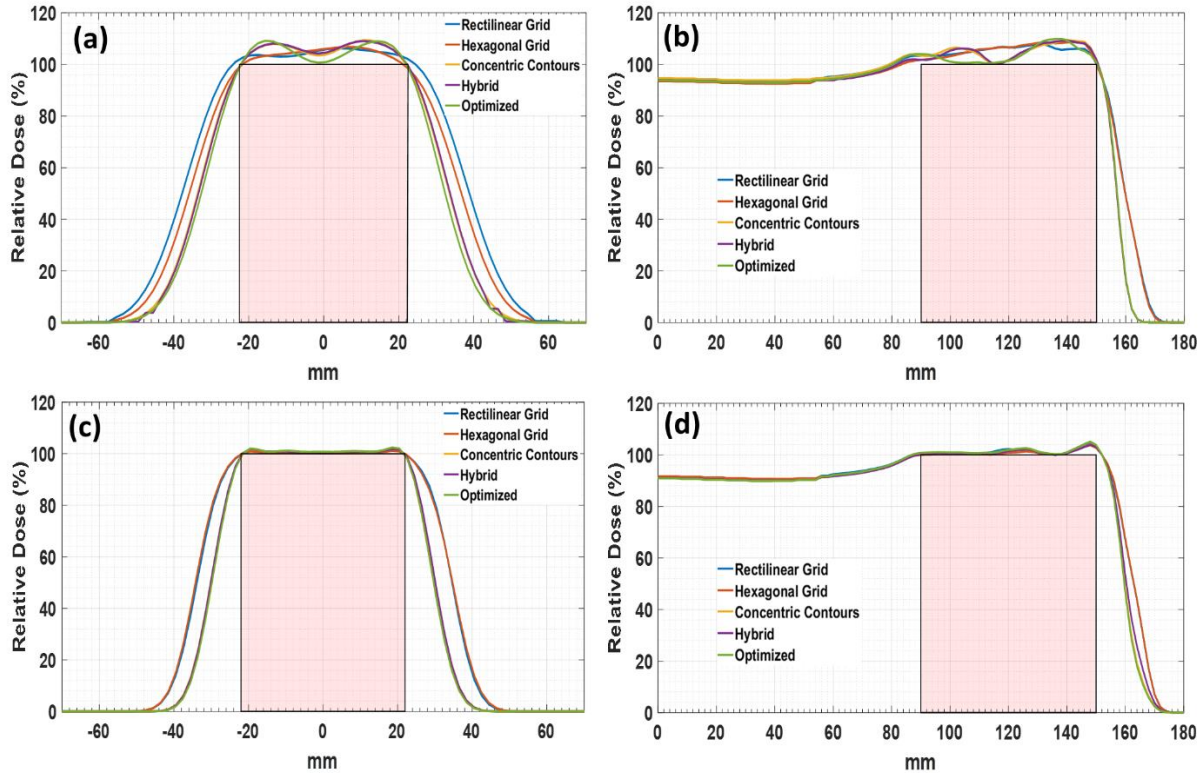

Figure 4.4: Lateral and central axis dose profiles for spherical target volume using medium spot size (row 1), small spot size (row 2) using different spot placement techniques

For conical target volume, this location corresponds to an energy layer of 121.77 MeV. The target volume corresponding to this particular energy layer is shown in Figure 4.5 (a). The spatial distribution of the spots for each spot placement technique at an energy layer of 121.77 MeV is shown in Figure 4.5 (b-f).

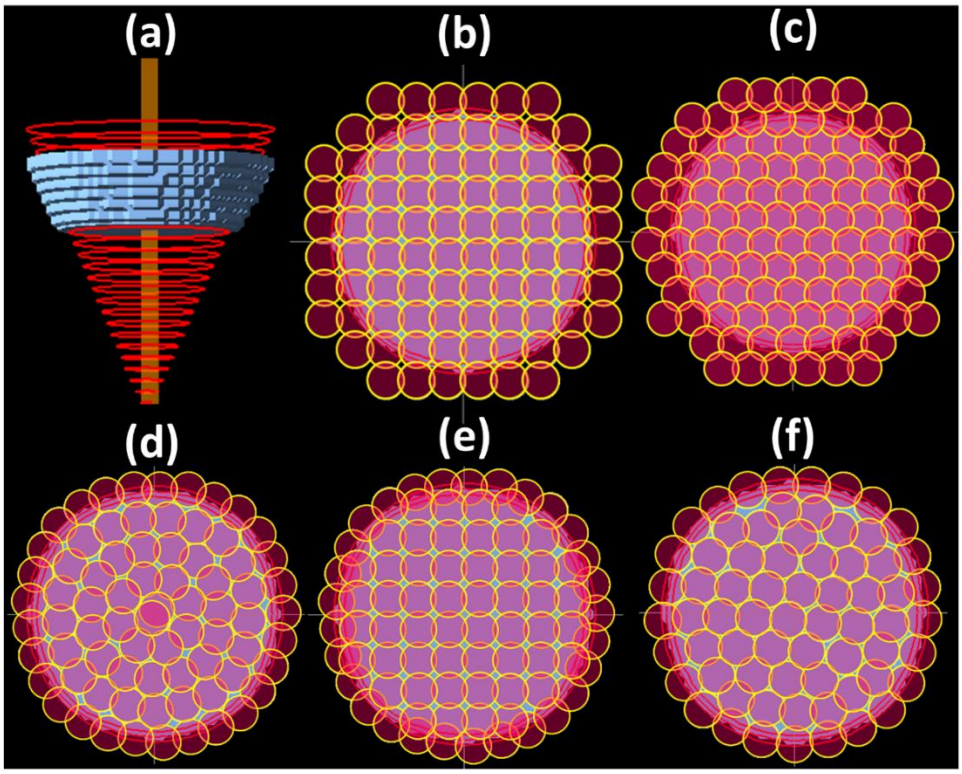

Figure 4.5: Spatial distribution of spots using all available spot placement techniques for the conical target volume at an energy of 121.77 MeV.

In case of boundary contoured spot placement techniques, the dose distributions (Figure 4.2) and dose profiles (Figure 4.3 and 4.4) for both target volumes represent reduced total dose to the normal tissues around the target volumes for both spot sizes. Tables 4.1 and 4.2 list the metrics computed for the spherical and conical target volumes, respectively, using all available spot placement techniques for medium and small spot sizes to highlight the important parameters for all spot placement techniques.

Table 4.1: Evaluation metrics for the spherical target volume using medium and small spot sizes for different spot placement techniques.

Spot Placement Technique	Spot Size (mm)	D_{max}(Gy)	Lateral Dose Falloff (mm)	Distal Dose Falloff (mm)	Conformity Index (CI)	Homogeneity Index (HI)	Integral Dose (Gy-L)	Spots Count
Rectilinear Grid	7.20	108.44	12.14	5.00	1.6	1.08	14.97	743
Hexagonal Grid	7.20	107.8	12.12	5.04	1.6	1.08	15.24	1116
Concentric Contours	7.20	109.9	10.98	5.10	1.58	1.1	14.16	425
Hybrid	7.20	109.82	11.00	5.07	1.56	1.1	14.16	510
Optimized	7.20	109.10	10.93	5.10	1.57	1.09	14.16	476
Rectilinear Grid	3.50	109.54	5.9	5.36	1.45	1.10	10.34	4215
Hexagonal Grid	3.50	109.77	5.82	4.91	1.44	1.10	10.34	4865
Concentric Contours	3.50	108.22	6.08	4.92	1.45	1.08	10.62	1988
Hybrid	3.50	108.31	5.89	5.19	1.44	1.08	10.34	2110
Optimized	3.50	108.79	5.96	4.92	1.44	1.09	10.34	1707

Table 4.2: Evaluation metrics for the conical target volume using medium and small spot sizes for different spot placement techniques.

Spot Placement Technique	Spot Size (mm)	D_{max}(Gy)	Lateral Dose Falloff (mm)	Distal Dose Falloff (mm)	Conformity* Index (CI)	Homogeneity Index (HI)	Integral Dose (Gy-L)	Spots Count
Rectilinear Grid	7.20	108.85	13.30	4.90	2.47	1.09	70.51	580
Hexagonal Grid	7.20	109.83	13.02	4.95	2.15	1.10	65.88	602
Concentric Contours	7.20	110.60	10.90	2.71	2.11	1.11	54.99	394
Hybrid	7.20	110.56	11.05	2.70	2.01	1.11	54.72	420
Optimized	7.20	110.12	11.80	2.67	1.99	1.10	57.71	358
*The value of CI is towards higher level because of the use of single field for a larger volume								
Rectilinear Grid	3.50	105.06	8.75	9.61	1.94	1.05	51.72	1799
Hexagonal Grid	3.50	104.06	9.46	9.52	1.95	1.04	52.27	2136
Concentric Contours	3.50	106.74	7.99	7.25	1.74	1.07	42.74	1393
Hybrid	3.50	107.12	7.79	8.37	1.74	1.07	42.47	1459
Optimized	3.50	108.41	7.88	7.13	1.74	1.08	41.92	1223

The lateral and distal falloff is either improved for boundary contoured spot placement techniques or remains consistent with the grid-based spot placement techniques. The concentric contours show a level of decreased dose homogeneity inside the spherical target volume while hybrid and optimized techniques slightly improve the homogeneity. There is a clear reduction in the total number of spots required for treatment of the whole target volume for all boundary contoured techniques (Table 4.1 & 4.2). While clear improvements are shown for the medium spot size for both spherical and conical target volumes, the impact on treatment plan quality is much less pronounced for the small spot size cases.

4.4 Discussion

By using the optimized spot placement technique, we find a clear reduction in the dose outside of the target volume shown in Figure 4.2. Using grid-based spot placement techniques, the dose falloff is inferior compared to the boundary contoured spot placement techniques in both lateral and distal ends of the target. For the conical target volume, lateral dose falloff, conformity index, and total dose to the normal tissue is improved for the medium spot size, but at the cost of increased maximum dose inside the target volume. The conical target volume has allowed us to highlight several important considerations when using large/medium spot sizes in PBS proton therapy, such as the ability to improve conformality and reduce spot counts by use of boundary contoured spot placements.

Figure 4.2 also explains the reason we chose conical shaped target volume where we can see the stair steps of the dose along the side of the cone in grid based as well as in other boundary contoured spot placement techniques when using the medium spot size. However, there is a linear

change in the dose falloff region in case of the optimized spot placement technique. In case of grid-based spot placement techniques, whenever there is an increase in tumor size for an energy layer, we have to add a whole row/column of spots to provide full tumor coverage on that layer. This change becomes more prominent when there is a sudden change in the structure. In case of conical shaped target, the shape (boundary) is changing slowly at every step. This causes the interior dose to be non-uniform. In order to bring it to the optimal level, we examine the stair steps in the dose falloff region. Even with the conc. contours and hybrid, there are still quantized jumps of the dose along the boundary of the cone. For example, from the tip of the cone, there may be one ring of the spots and as we go up, we go from two rings of spots to three rings of spots and so on. That in turn causes the inside dose to be non-uniform and in order to get that level of uniformity inside, we examine the stair steps at the boundary.

Figure 4.2 also shows a modest improvement in case of optimized spot placement technique. It can be seen that the dose has a smooth linear slope for the whole target volume. Using the grid-based spot placement techniques, if TPS do not reset the grid, whenever the shape changes, the conformality suffers for that energy layer. The treatment plans created using optimized spot placement techniques provide a conformal dose distribution to the target volume. This was one of the objectives of performing this study in 3D and selecting a conical target volume was to highlight this important aspect of the spot placement techniques that is obvious in Figure 4.2 for the optimized spot placement technique using medium spot size.

However, the use of smaller spot sizes can provide an improvement in the overall treatment plan quality but by using the optimized spot placement technique, fewer spots can be utilized to get the same results for a treatment plan. Using the smaller spot size, the treatment plan quality can be

improved but an important factor of treatment time should also be considered as using smaller spot sizes can increase the treatment time [21]. Like the other treatment planning parameters, the spot placement technique is also an important treatment planning parameter. The optimized spot placement technique can provide highly conformal treatment plans for arbitrary tumor geometries.

CHAPTER 5: CONCLUSION AND FUTURE WORK

Much effort has been expended recently in an attempt to improve plan quality in proton PBS treatments and several gains have been made by efforts such as spot size reduction and development of advanced movable proton collimator systems [18, 21, 23, 26, 44, 45]. However, these approaches may come with an increased cost, an increase in delivery times [21, 23, 26, 27, 36] and/or with added neutron dose contamination [27, 36, 44].

In this work, an optimized spot placement technique has been proposed as an alternative to the commercially available one that can provide a geometrically robust spot distribution for arbitrarily complex target shapes in proton pencil beam scanning.

This technique along with the other boundary contoured spot placement techniques (concentric contours and hybrid) were tested and dosimetric comparisons were made. It highlights key features of different spot placement techniques. The dose distribution and quantitative analysis of lateral and depth dose distributions have shown that the optimized spot placement technique can provide improved normal tissue sparing, as compared to the conventional grid-based spot placement techniques. It has demonstrated a robust spot distribution inside the target that can provide an attractive, low-cost option to improve proton PBS plan quality without added cost and with a potential decrease in delivery times due to the reduction in spot count.

It is believed that future work that extends this approach to include clinically important three dimensional effects, such as finite layer width (i.e. Bragg Peak width), range uncertainty, and setup uncertainty, will showcase the clinical benefit of having the highly uniform planar spot distributions that the newly proposed spot placement technique has been shown to produce.

This work also shows that substantial patient benefit can be realized without the need for major equipment upgrades, such as would be required to reduce spot sizes or incorporate complex movable collimators (although such approaches can be used in conjunction with this approach to achieve even greater benefits). Overall, this work has provided a foundational new approach to spot placement in proton PBS treatments that will enable future studies to quantify the full benefit to patients, while incorporating practical considerations such as tissue heterogeneity and plan robustness.

APPENDIX: LIST OF PUBLICATIONS

Mahboob ur Rehman, Kevin Erhart, Jerrold Kielbasa, Sanford L. Meeks, Zhiqiu Li, Twyla Willoughby, Naren Ramakrishna, Ken Stephenson, Talat S. Rahman, Patrick Kelly, Omar Zeidan *"An Optimized Approach for Robust Spot Placement in Proton Pencil Beam Scanning"* Phys Med Biol. 2019; 64(23): 235016. Published 2019 Dec 5. doi:10.1088/1361-6560/ab4e78

In Preparation

Mahboob ur Rehman, Omar A. Zeidan, Twyla Willoughby, Sanford L. Meeks, Patrick Kelly, Kevin Erhart *"Dosimetric impact of using different spot placement techniques in proton pencil beam scanning."*

LIST OF REFERENCES

[1] https://www.who.int/news-room/fact-sheets/detail/cancer

[2] https://www.ptcog.ch/index.php/facilities-in-operation

[3] R.R. Wilson, Radiological use of fast protons, Radiology 47 (1946) 487-491.

[4] W.D. Newhauser, R. Zhang, The physics of proton therapy, Physics in Medicine & Biology 60 (2015) R155.

[5] C. Tobias, J. Lawrence, J. Born, R. McCombs, J. Roberts, H. Anger, B. Low-Beer, C. Huggins, Pituitary irradiation with high-energy proton beams a preliminary report, Cancer research 18 (1958) 121-134.

[6] P. ICRU, Recording, and ReportingProton-Beam Therapy (ICRU Report 78), Journal of the ICRU 7 (2007).

[7] H. Paganetti, Proton therapy physics, CRC press2018.

[8] J. Deasy, ICRU Report 49, stopping powers and ranges for protons and alph particles, Wiley Online Library, 1994.

[9] K. Langen, M. Mehta, Proton Beam Therapy Basics, Journal of the American College of Radiology 12 (2015) 1204-1206.

[10] R.V. Sethi, H.A. Shih, D. Kim, B.Y. Yeap, K. Mouw, K.C. Marcus, E. Grabowski, T.I. Yock, N. Tarbell, S. Mukai, Second non-ocular tumors among survivors of retinoblastoma treated with proton therapy, American Society of Clinical Oncology, 2013.

[11] F.H. Attix, Introduction to radiological physics and radiation dosimetry, John Wiley & Sons2008.

[12] N. Bohr, II. On the theory of the decrease of velocity of moving electrified particles on passing through matter, The London, Edinburgh, and Dublin Philosophical Magazine and Journal of Science 25 (1913) 10-31.

[13] C. Edwards, Fundamental quantities and units for ionizing radiation—ICRU report 60, Elsevier, 1999.

[14] H. Bethe, Zur theorie des durchgangs schneller korpuskularstrahlen durch materie, Annalen der Physik 397 (1930) 325-400.

[15] F. Bloch, Zur bremsung rasch bewegter teilchen beim durchgang durch materie, Annalen der Physik 408 (1933) 285-320.

[16] A. Elia, Characterization of the GATE Monte Carlo platform for non-isocentric treatments and patient specific treatment plan verification at MedAustron-Vienna-Austria, Université de Lyon, 2019.

[17] B.R. Smith, D.E. Hyer, P.M. Hill, W.S. Culberson, Secondary neutron dose from a dynamic collimation system during intracranial pencil beam scanning proton therapy: a Monte Carlo investigation, International Journal of Radiation Oncology* Biology* Physics 103 (2019) 241-250.

[18] J. Alshaikhi, P.J. Doolan, D. D'Souza, S.M. Holloway, R.A. Amos, G. Royle, Impact of varying planning parameters on proton pencil beam scanning dose distributions in four commercial treatment planning systems, Medical physics 46 (2019) 1150-1162.

[19] E. Pedroni, R. Bacher, H. Blattmann, T. Böhringer, A. Coray, A. Lomax, S. Lin, G. Munkel, S. Scheib, U. Schneider, The 200‐MeV proton therapy project at the Paul Scherrer Institute: Conceptual design and practical realization, Medical physics 22 (1995) 37-53.

[20] U. Titt, D. Mirkovic, G.O. Sawakuchi, L.A. Perles, W.D. Newhauser, P.J. Taddei, R. Mohan, Adjustment of the lateral and longitudinal size of scanned proton beam spots using a pre-absorber to optimize penumbrae and delivery efficiency, Physics in Medicine & Biology 55 (2010) 7097.

[21] A.C. Kraan, N. Depauw, B. Clasie, M. Giunta, T. Madden, H.M. Kooy, Effects of spot parameters in pencil beam scanning treatment planning, Medical physics 45 (2018) 60-73.

[22] G. Meier, D. Leiser, R. Besson, A. Mayor, S. Safai, D.C. Weber, A.J. Lomax, Contour scanning for penumbra improvement in pencil beam scanned proton therapy, Physics in Medicine & Biology 62 (2017) 2398.

[23] M. Moteabbed, T.I. Yock, N. Depauw, T.M. Madden, H.M. Kooy, H. Paganetti, Impact of spot size and beam-shaping devices on the treatment plan quality for pencil beam scanning proton therapy, International Journal of Radiation Oncology* Biology* Physics 95 (2016) 190-198.

[24] H. Paganetti, Proton therapy physics, CRC Press2016.

[25] M. ur Rehman, K. Erhart, J. Kielbasa, S.L. Meeks, Z. Li, T. Willoughby, N. Ramakrishna, K. Stephenson, T.S. Rahman, P. Kelly, An optimized approach for robust spot placement in proton pencil beam scanning, Physics in Medicine & Biology 64 (2019) 235016.

[26] D. Wang, B. Dirksen, D.E. Hyer, J.M. Buatti, A. Sheybani, E. Dinges, N. Felderman, M. TenNapel, J.E. Bayouth, R.T. Flynn, Impact of spot size on plan quality of spot scanning proton radiosurgery for peripheral brain lesions, Medical physics 41 (2014).

[27] D.E. Hyer, P.M. Hill, D. Wang, B.R. Smith, R.T. Flynn, Effects of spot size and spot spacing on lateral penumbra reduction when using a dynamic collimation system for spot scanning proton therapy, Physics in Medicine & Biology 59 (2014) N187.

[28] J. Saini, N. Cao, S.R. Bowen, M. Herrera, D. Nicewonger, T. Wong, C.D. Bloch, Clinical commissioning of a pencil beam scanning treatment planning system for proton therapy, International journal of particle therapy 3 (2016) 51-60.

[29] W. Chen, D. Craft, T.M. Madden, K. Zhang, H.M. Kooy, G.T. Herman, A fast optimization algorithm for multicriteria intensity modulated proton therapy planning, Medical physics 37 (2010) 4938-4945.

[30] Y. Mori, The Current Status of Proton Beam Therapy, Proton Beam Radiotherapy, Springer2020, pp. 23-33.

[31] S. Rana, A.B. Rosenfeld, Parametrization of in-air spot size as a function of energy and air gap for the ProteusPLUS pencil beam scanning proton therapy system, Radiological Physics and Technology 13 (2020) 392-397.

[32] S. Rana, O. Zeidan, E. Ramirez, M. Rains, J. Gao, Y. Zheng, Measurements of lateral penumbra for uniform scanning proton beams under various beam delivery conditions and comparison to the XiO treatment planning system, Medical physics 40 (2013) 091708.

[33] T.F. De Laney, H.M. Kooy, Proton and charged particle radiotherapy, Lippincott Williams & Wilkins2008.

[34] B. Clasie, A. Wroe, H. Kooy, N. Depauw, J. Flanz, H. Paganetti, A. Rosenfeld, Assessment of out-of-field absorbed dose and equivalent dose in proton fields, Medical physics 37 (2010) 311-321.

[35] H.M. Kooy, B.M. Clasie, H.-M. Lu, T.M. Madden, H. Bentefour, N. Depauw, J.A. Adams, A.V. Trofimov, D. Demaret, T.F. Delaney, A case study in proton pencil-beam scanning delivery, International Journal of Radiation Oncology* Biology* Physics 76 (2010) 624-630.

[36] D.E. Hyer, P.M. Hill, D. Wang, B.R. Smith, R.T. Flynn, A dynamic collimation system for penumbra reduction in spot-scanning proton therapy: Proof of concept, Medical physics 41 (2014) 091701.

[37] D. Wang, B. Dirksen, D.E. Hyer, J.M. Buatti, A. Sheybani, E. Dinges, N. Felderman, M. TenNapel, J.E. Bayouth, R.T. Flynn, Impact of spot size on plan quality of spot scanning proton radiosurgery for peripheral brain lesions, Medical physics 41 (2014) 121705.

[38] L. Lin, C.G. Ainsley, J.E. McDonough, Experimental characterization of two-dimensional pencil beam scanning proton spot profiles, Physics in Medicine & Biology 58 (2013) 6193.

[39] A.J. Lomax, T. Böhringer, A. Bolsi, D. Coray, F. Emert, G. Goitein, M. Jermann, S. Lin, E. Pedroni, H. Rutz, Treatment planning and verification of proton therapy using spot scanning: initial experiences, Medical physics 31 (2004) 3150-3157.

[40] C. Winterhalter, G. Meier, D. Oxley, D.C. Weber, A.J. Lomax, S. Safai, Contour scanning, multi-leaf collimation and the combination thereof for proton pencil beam scanning, Physics in Medicine & Biology 64 (2018) 015002.

[41] Q. Du, M. Emelianenko, L. Ju, Convergence of the Lloyd algorithm for computing centroidal Voronoi tessellations, SIAM journal on numerical analysis 44 (2006) 102-119.

[42] S. Lloyd, Least squares quantization in PCM, IEEE transactions on information theory 28 (1982) 129-137.

[43] .decimal App Documentation, 2021.

[44] B.-H. Chiang, A. Bunker, H. Jin, S. Ahmad, Y. Chen, Developing a Monte Carlo model for MEVION S250i with HYPERSCAN and Adaptive Aperture™ pencil beam scanning proton therapy system, Journal of Radiotherapy in Practice (2020) 1-8.

[45] A. Moignier, E. Gelover, D. Wang, B. Smith, R. Flynn, M. Kirk, L. Lin, T. Solberg, A. Lin, D. Hyer, Theoretical benefits of dynamic collimation in pencil beam scanning proton therapy for brain tumors: dosimetric and radiobiological metrics, International Journal of Radiation Oncology* Biology* Physics 95 (2016) 171-180.